Dynamic Nanoparticle Assembly and its Application in Stimuli Responsive Drug Delivery

A Thesis

Submitted in Partial fulfilment for the degree of

Master of Science

as a part of

Integrated Ph.D Programme (Chemical Science)

By

Mr. Santu Sinha

New Chemistry Unit

Jawaharlal Nehru Centre for Advanced Scientific Research

(A Deemed University)

Bangalore – 560064 (INDIA)

March - 2018

Declaration

I here by declare that matter embodied in the thesis entitled **"Dynamic Nanoparticle Assembly and its Application in Stimuli Responsive Drug Delivery"** is the result of the research carried out by me at the New Chemistry Unit, Jawaharlal Nehru Centre for Advanced Scientific Research, Bangalore, India. This work is done under the supervision of **Dr. Sarit S. Agasti** and it has not been submitted elsewhere for the award of any degree or diploma.

In keeping with the general practice in reporting the scientific observations, due acknowledgement has been made whenever the work described is based on the findings of other fellow researchers. Any omission that might have occurred due to oversight or error is regretted.

_____

Mr. Santu Sinha

(Int.Ph.D Student)

Certificate

I here by declare that the matter embodied in the thesis entitled **"Dynamic Nanoparticle Assembly and its Application in Stimuli Responsive Drug Delivery"** has been carried out by Mr. Santu Sinha at the New Chemistry Unit, Jawaharlal Nehru Centre for Advanced Scientific Research, Bangalore, India under my supervision and it has not been submitted elsewhere for the award of any degree or diploma.

_____

Dr. Sarit S. Agasti

(Research Supervisor)

Acknowledgements

First and foremost, I would like to express my sincere gratitude to my supervisor, Dr. Sarit S. Agasti, Faculty Fellow, JNCASR Programmable Molecular Design Laboratory, New Chemistry Unit, JNCASR who right from the beginning of my project provided me with all the facilities to carry out my research and monitored my work.

I would like to thank Professor C. N. R. Rao, FRS for his support and encouragement throughout my stay in JNCASR. His presence has given me immense inspiration to indulge in active research. I also thank him for providing the infrastructure and facilities to carry out my research work at NCU, JNCASR.

I would like to thank all my course instructor for the valuable courses which were extremely helpful to me.

I am gratefull to all my past and present lab members – Ranjan Sasmal, Dr. Shafeekh K methal, Meenakshi Pahwa. Arka Som, Dr. Nilanjana Das Saha, Preethi V. G, Soumya C, Shashidhara Pura, Manideepa Dhar for their help in various capacities, co-operation and maintaining cheerful atmosphere in the lab.

I would like to express my sincere thanks to all the academic, administrative, security, library, comp-lab and Dhanvantri staffs for making our campus life smooth and easy.

Table of contents

Introduction

Chapter 1: Stimuli responsive dynamic nanoparticle assembly

1.1 Introduction to dynamic nanoparticle assembly

Nature has continuously amaze material scientists with her ability to create intelligent living things using techniques of self-assembly.[1] Nature provides many examples of complex, highly organised self-assembled structures.[1] For instance, bird homing ability of migratory birds (including homing pigeons, domestic chickens) also guided by magnetic nanoparticle (NP) assemblies found in the upper beak skin of this birds.[1] Also assembled magnetic nanoparticles found in the nasal capsule of sea salmon is sensitive to the geomagnetic field and help in guiding their journeys in the endless ocean.[1] Inspired from this natural instance, material scientists (including nanomaterial scientists) have also tried to developed several assembly processes to create artificial smart materials.[2,3,4,5] Nanoparticle assemblies exhibit physical and chemical properties, which are different from those of both individual nanoparticles and their bulk aggregates.[4]

Dynamic NP assemblies are spontaneously formed superstructures made of more than two nanoscale particles that show the ability to alter their geometrical, physical and other properties.[6] This process is often driven by both interparticle interactions and the influence of the assembly environment.[6] The dynamic nanoparticle assemblies is considered as one type of nanoarchitectonics which are based on ligand assisted functionalization.[1] NP assemblies exhibit physical and chemical properties, which are different from those of both individual NPs and

their bulk aggregates.[6] Importantly “smart” materials with programmed responses to external stimuli can be designed based on assembly of NPs assisted by their surface ligands for different biomedical applications.[1] This NP assemblies can be made responsive by exogenous stimuli (like, to magnetic field, temperature, ultrasound, light, or electric pulses) or endogenous stimuli (to pH, enzymatic activity, or redox gradients). [1,6,7] These dynamic nanoparticle assemblies offer a new platform for constructing stimuli responsive materials with enhanced functionalities, which can meet the fast-growing needs of the modern medicine. [1]

1.2 Applications of dynamic nanoparticle assembly

Dynamic nanoparticle (NP) assemblies present new possibilities for constructing adaptive systems, devices and smart materials that can incorporate both nanoscale and molecular functional components.[8] Dynamic nanoparticle assembly shows very good potential to reveal fundamental insights about dynamic and complex chemical systems confined to nanoscale interfaces.[8] Scientists in the different area of research have already demonstrated the different application of this dynamic process ranging from materials to biology.[9] Here are some essential and recent examples of the application based on dynamic nanoparticle assembly. [9,10,11,12,13]

1.2.1 Application in materials

Application of dynamic nanoparticle assembly in materials research has been implemented in the development of reconfigurable crystals and separation of organic molecules from solution, etc.[10,11] Development of crystal with different configuration are required for the generation of materials with different optical properties.[11] The optical properties of the NPs depend on the number and the proximity of the NPs present.[4] Mirkin and coworkers have demonstrated one example of reconfigurable crystal based on the dynamic NP system with the aid of DNA nanotechnology.[11] They developed system constructed by transmutable NP, which is a gold NP functionalized with DNA hairpin. This transmutable nanoparticle undergoes transition into two different states on the addition of effector strand and protector strand (Fig. 1.1). Effector strand binds with the loop of the hairpin and makes it unfolded, which makes the sticky end of DNA hairpin get exposed. On the other hand, protector strand removes the effector strand by strand displacement reaction and hairpin again gets refolded and thereafter the sticky end gets buried in the core of ligand monolayer. In the unfolded state of the hairpin, as the sticky ends get exposed to each other, NPs can bind to each other and form the crystal through the favourable interaction of DNA hybridisation. For NPs functionalized with two orthogonal hairpins, effector and protector strands are orthogonal so that hairpin can be activated separately in the desired fashion. For

activation of hairpin having a self-complementary relationship, crystal structure of FCC observed (Fig. 1.2). Crystal converted to BCC by disrupting the initial interaction (by protector strand), the NP comes to the dispersed state, then through applying another effector strand, another hairpin gets unfolded which leads to NPs to crystallise in BCC. Here DNA has been used as external triggered to drive the process.

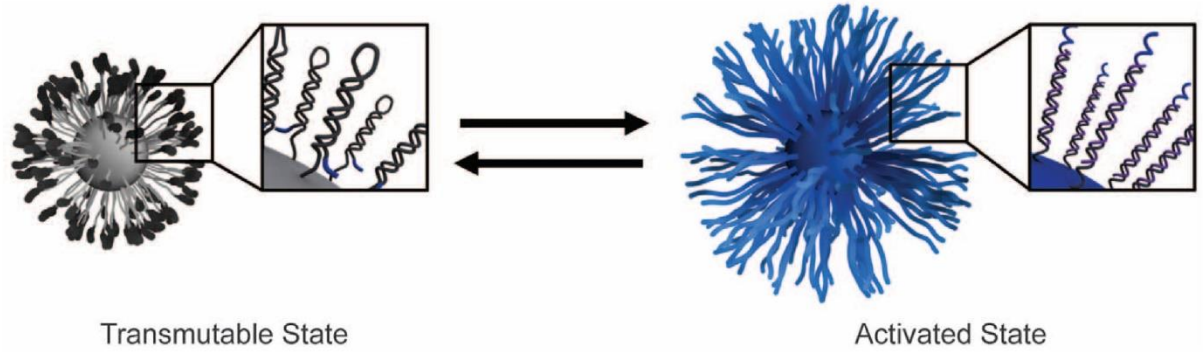

Fig. 1.1 | Reversible transition of nanoparticle between transmutable state and activated state. Activation of transmutable nanoparticle based on the unfolding of DNA hairpin reversibly on the surface of nanoparticles. Reproduced with permission.[11] Copyright 2016, AAAS.

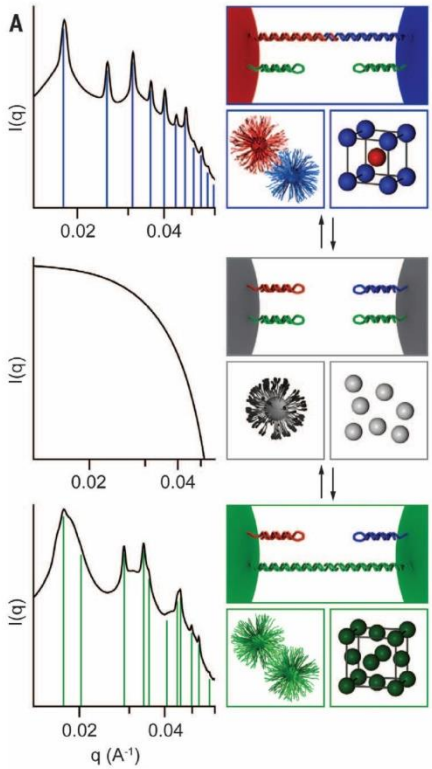

Fig. 1.2 | Dynamic reconfigurable crystal made by DNA-NP, crystal transition happened reversibly between BCC and FCC through a non-crystalline dispersed state of nanoparticles. In activation of self-complementary hairpins (green colour) FCC structure was observed and folding of the same hairpin leaded particles to disperse. On the other hand, unfolding of non-self-complementary DNA hairpins (red and blue) BCC structure appeared. Reproduced with permission.[11] Copyright 2016, AAAS.

Dynamic NP assembly process was even designed in aiming for water purification purpose.[9] The process of assembly is very rapid in a manner so that we can be utilized this process for successful encapsulation of organic molecules from

solution.[9] Rafal klajn and coworkers have demonstrated reversible encapsulation and release of dye molecules from solution based on this dynamic assembly process.[9] Non-photoresponsive NPs were reversibly self-assembled within a photoswitchable medium by modulating the interparticle interactions. Nanoparticles functionalized with pH sensitive –COOH group self-assembled in basic pH medium due to intermolecular hydrogen bonding between NPs (Fig. 1.3**)**. Here light has been used as an external trigger to assemble and disassemble NPs with the aid of pH switching mechanism by using a photoacid as an internal regulator. Here photo acid changes (protonated merocyanine (MCH+)) the pH of the medium reversible by applying UV light. Blue light irradiation increased the acidity of the medium, leading to weakening of hydrogen bonds and disassembly of the NPs. However, in the dark or ambient conditions, the NPs spontaneously reassembled. This process of assembly and disassembly goes on continue for multiple cycles. In every cycle, the process efficiently captured dye molecules from the solution and released during disassembly. The process developed here shows reversible encapsulation and release of NBD dye molecule very efficiently (Fig. 1.4**)**.[9] This rapid and efficient cycling process of assembly and disassembly can be used in a similar way for the separation of the unwanted molecule from the solution by careful design of dynamic NP assembly decorated with the proper ligands.[9]

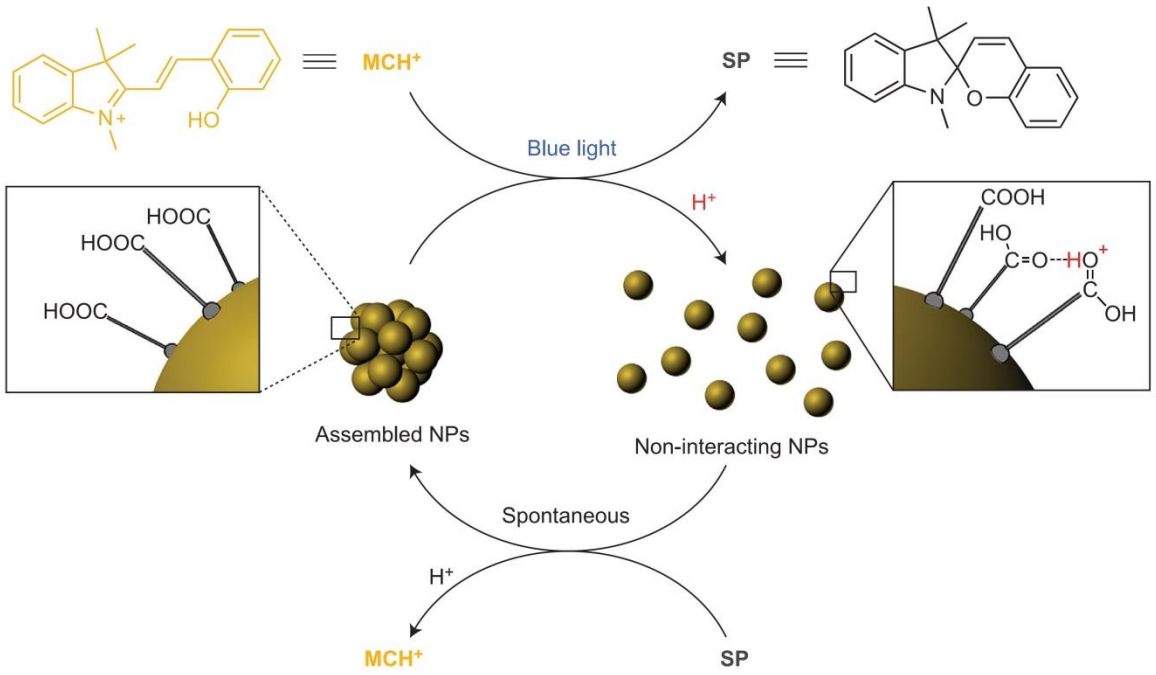

Fig. 1.3 | Light-controlled self-assembly of non-photoresponsive nanoparticles. Blue light leads the generation of the proton which hampers the interparticle interaction and finally the particle disassembles. Again, transition of merocyanine molecules from the cyclic unstable state (SP) to stable open form (MCH^+) abstract the proton from the medium and again interparticle hydrogen bonding formation leads particle to get self-assembled. Reproduced with permission.[9] Copyright 2015, Nature Publishing Group.

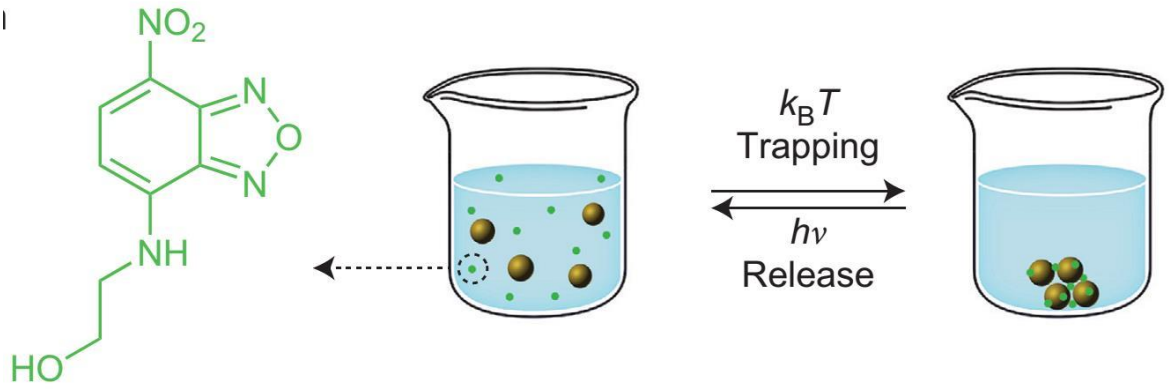

Fig. 1.4 | Reversible trapping and release of NBD dye molecules by photoresponsive dynamic NP assembly. Reproduced with permission.[9] Copyright 2015, Nature Publishing Group.

1.2.2 Application in catalysis of the reaction

Dynamic NP assembly process has the potential to be used for catalysis of different processes where no conventional catalyst is available for enhancing the reaction rate.[10] Rafal klajn and coworkers have developed a new approach of catalysis using the nano-hotspot of this dynamic process, named as 'nanoflask' (Fig. 1.6**)**.[10] During the process of assembly when nanometer-sized particles get aggregated to each other, there is generation of void space inside this assembly. Due to the dynamic nature of this system, the generated nanoflask was dynamic in nature and thus this was coined as 'dynamic nanoflask' regulated by light. The driving force behind this aggregation process is the photoinduced formation of Z-azobenzene at the NP surface, which leads to the entropically favoured release of nonpolar

solvent molecules (Fig. 1.5). The inner voids of the aggregates are ideally suited for use as tiny reaction vessels because they provide both sufficient space and specific interactions between the molecules and the 'nanoflask' walls.[10] The acceleration in the rate is due to an increased local concentration inside the 'nanoflasks' and an effectively reduced energy barrier, which arises from 'pumping' the system to metastable Z-azobenzene-containing aggregates.[10]

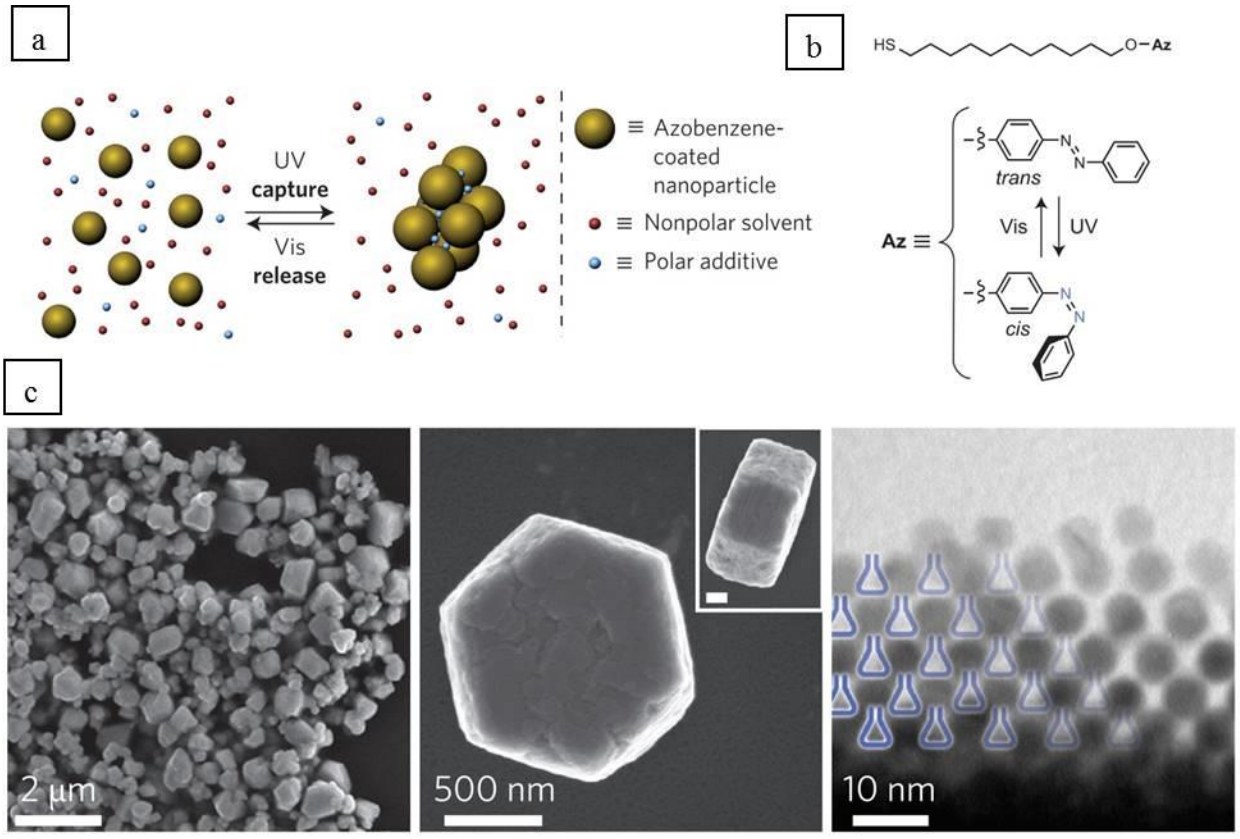

Fig. 1.5 | Reversible trapping and reaction acceleration within dynamic nanoparticle assembly (nanoflask). **a)** Reversible assembly of azobenzene-functionalized gold nanoparticles. **b)** Structure of the azo ligand and

photoisomerization of azobenzene by light. **c)** TEM images of nanoparticle assembly in increasing order of magnification. Higher magnified images shows nano hotspots between nanoparticles which acts as nano reactor vessel. Reproduced with permission.[10] Copyright 2016, Nature Publishing Group.

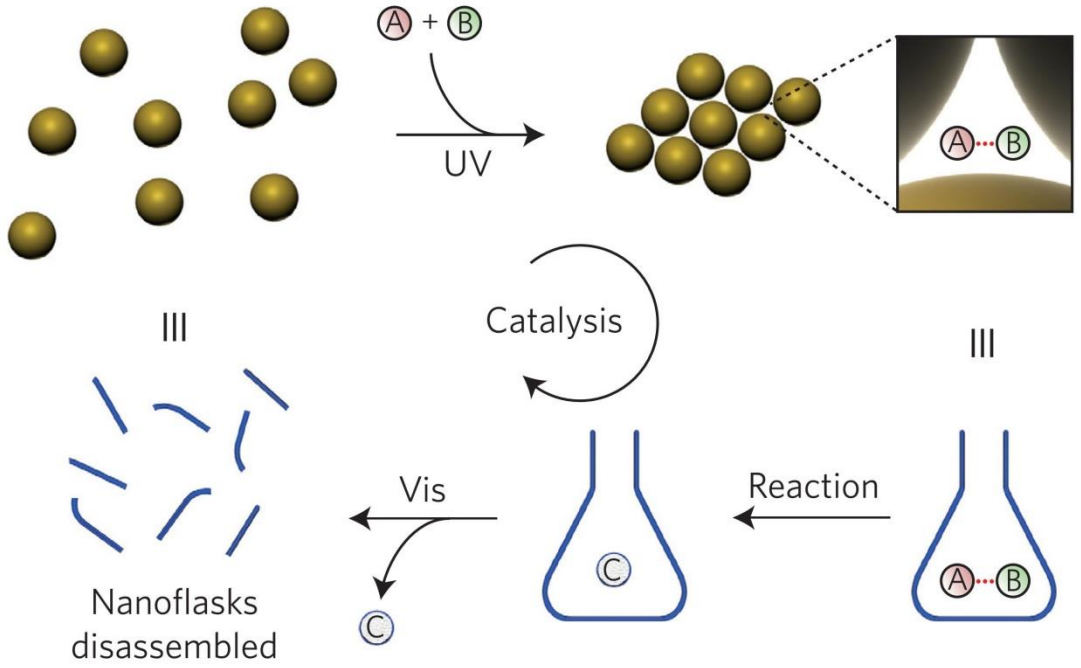

Fig. 1.6 | Schematic of encapsulation of reacting molecules during light directed assembly, ongoing reaction in nanoflask and further disassembly by visible light with the release of products from nanoflask. The overall process continues multiple times and leads efficient conversion of reactions. Reproduced with permission.[10] Copyright 2016, Nature Publishing Group.

1.2.3 Application in biology

Dynamic NP assembly also performs some essential biological applications such as artificial nanosystem of protein-like functions developed based on dynamic NP system.[12] Warren chan and coworkers reported a DNA-strand-triggered dynamic NP assembly as a differential cell-targeting system. AuNPs with three different sizes (13 nm, 6 nm, and 3 nm) were modified with two types of thiolated DNAs on each type of particles.[12] Two linker DNAs, which were designed to link 13 nm (NP1) AuNP with 3 nm (L1) and 6 nm (NP2) AuNPs. When two linker respectively were added into the mixture of the above three groups of AuNPs, the NP gets assembled and a core-satellite structure forms, as shown in (Fig. 1.7**)**.[12] When linker A1 is added, 3 nm AuNP and 6 nm AuNP were bridged. When DNA sequence $L1_{comp}$ is added, it takes out the L1 DNA by strand displacement reaction, therefore interaction between NP1 and 3nm NP breaks and all the smaller NP gets transferred from the surrounding of 13 nm NP the to surroundings of 6nm.[12] The reverse process is also possible by applying DNA of proper sequence in proper order. For the transition from morphology-2 to morphology-1, the system goes through the same intermediate state. On addition of L1 strand in morphology-1, NP1 again gets connected to the smaller NP, thereby forming the intermediate structure. Now the addition of $A1_{comp}$ takes out the A1 strand from the assembly by DNA strand displacement reaction. As A1 is not there, so interaction between NP2

and smaller NP breaks and all the smaller NPs get transferred from surroundings of NP2 to the surroundings of NP1.[12] TEM has characterized this morphological transition of dynamic NP system, showing the proposed transition of satellite NP from one core NP to another core NP. Further, they developed this dynamic NP assembly as a differential cell targeting system that can be useful for different drug delivery purpose.[12]

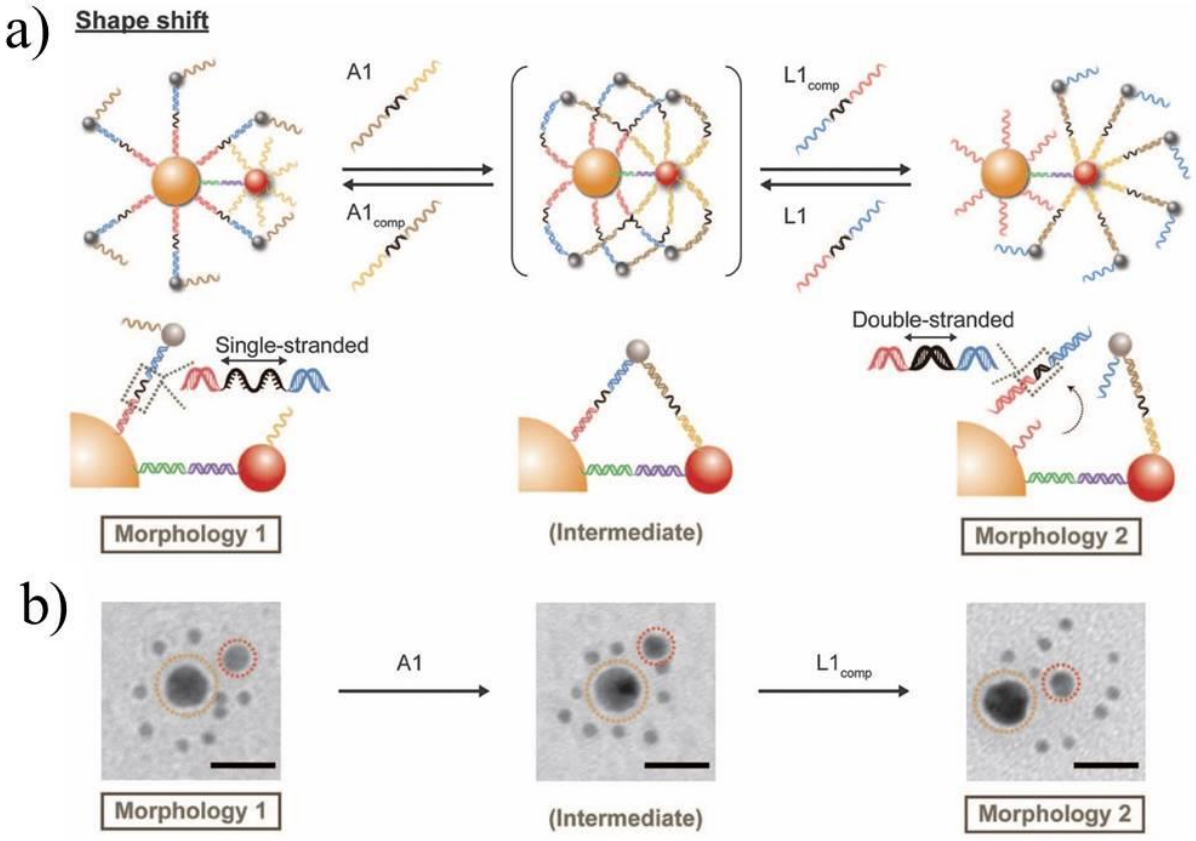

Fig. 1.7 | DNA directed dynamic nanoparticle assembly. **a)** Schematic of transition of nanoparticle assembly from morphology-1 to morphology-2 through an intermediate bridge state. All smaller satellite nanoparticle (3-nm) undergo a place

alternation from the site of bigger nanoparticle (13-nm, NP1) to the site of medium size nanoparticle (6-nm, NP2) through a series of DNA hybridization and strand displacement reaction. **b)** TEM images of morphology-1 and intermediate state on the addition of linker DNA strand A1 and morphology-2 on the addition of $L1_{comp}$ strand which breaks the linking between NP1 and smaller nanoparticles by strand displacement reaction. Reproduced with permission.[12]Copyright 2016, AAAS.

This dynamic transition of smaller NP covers the surroundings of the NP1 reversibly. The second trick involves the addition of targeting ligands folic acid to the surface of NP1. In morphology all small NPs cover the targeting ligand and entire the NP remain in nonadhesive state. In the presence of the appropriate linker and detachment oligonucleotides, long DNA is moved to NP2, and the targeting ligands on the surface of NP1 become accessible. The entire NP is in the adhesive state and can specifically bind to cells expressing the receptor for the targeting ligand, and is then incorporated into cells via receptor-mediated endocytosis (Fig. 1.8). When this two different morphologies were treated with the cells, they showed different extent of cellular internalization, as characterized by TEM of cell treated with folic acid functionalized NP assembly. In morphology-1, all the folic acid targeting ligand are covered by smaller NPs and are not accessible for interaction with the cell surface, hence they interact less with the cells leading to low cellular internalization. In morphology-2, all folic acid targeting ligands are on

the NP1 surface and are free to interact with the cell surface without any interruption, therefore interaction with cell surface is more and thus show higher cellular internalization.[12]

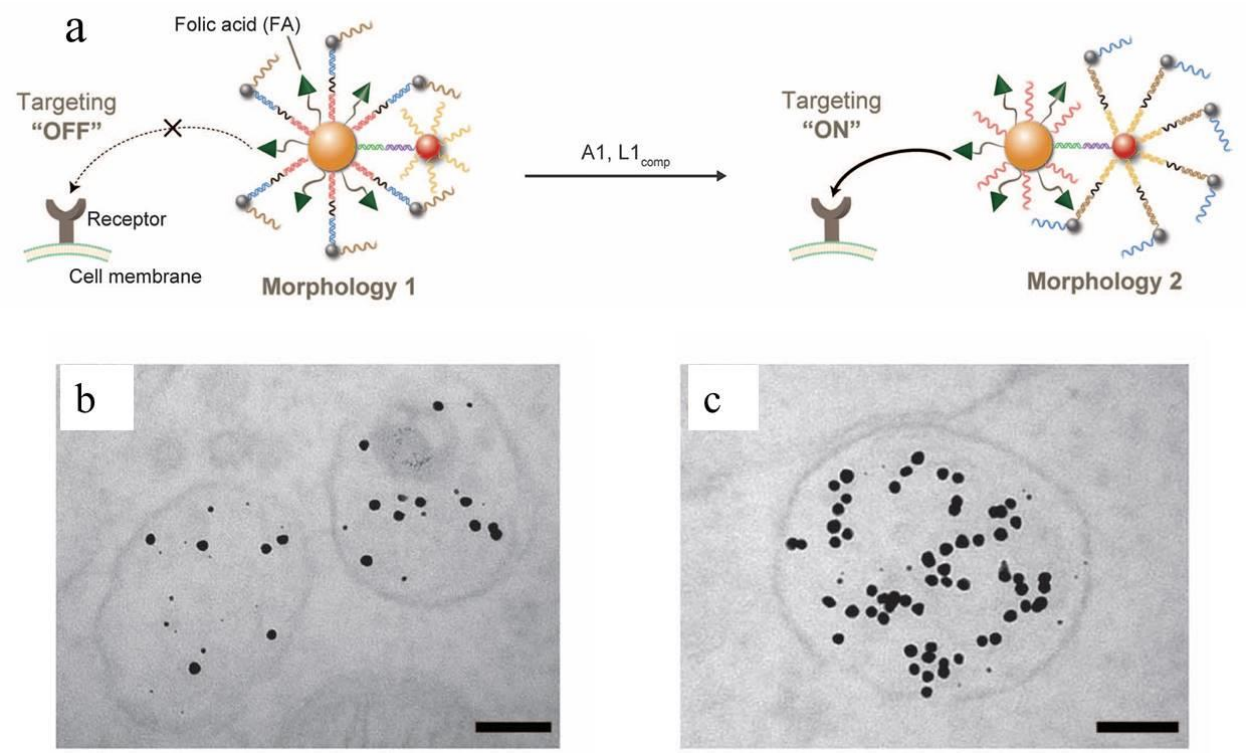

Fig. 1.8 | Differential cellular interaction of dynamic nanoparticle assembly. **a)** Assembly in morphology-1 state cannot interact with the cell surface as targeting ligands are not accessible and in the morphology-2 state, the assembly can interact with the cell surface very efficiently. **b)** TEM of cellular uptake of morphology-1 shows less nanoparticle inside the cell. **c)** TEM of cellular uptake of morphology-2 shows higher number of nanoparticles inside the cell. Reproduced with permission.[12]Copyright 2016, AAAS.

1.3 Introduction to the bio-orthogonal host-guest interaction of CB[7] and ADA

Cucurbit[n]urils are macrocyclic molecule consist of glycoluril molecules bound in a ring-like arrangement via methylene bridges containing two portals.[13,14,15,16,17,18] Portal size and cavity volume of cucurbit[n]urils increases with increase in number of glycouril molecules. Comparison of some structural parameters of CB[n] given in Fig. 1.10. On moving from CB[5] to CB[8], the mean diameter of the internal cavity increases from 4.4 to 8.8 Å and mean diameter of portal also increases from 2.4 to 6.9 Å. X-ray crystal structure also reveals the similar trend of increase in cavity size from CB[5] to CB[8](Fig 1.9). Both the rich hydrogen-bonding ability and ion-dipole interactions of the portals and the covalent rigidity of the host, contribute to the chemistry of these compounds.The solubility of CB homologues in common solvents is also low ($<10^{-5}$ M), except that CB[5] and CB[7] have a moderate solubility in water ($2\text{-}3x10^{-2}$ M).

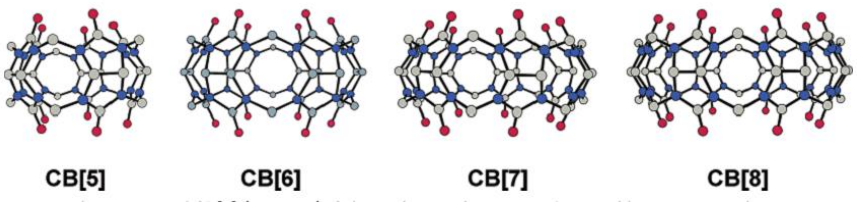

Fig. 1.9 | X-ray crystal structures of CB[n](n)5-8). Colour codes: carbon, grey; nitrogen, blue; oxygen, red. Reproduced with permission.[16] Copyright 2003, ACS.

Chart 1

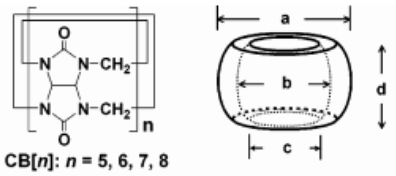

CB[*n*]: *n* = 5, 6, 7, 8

		CB[5]	CB[6]	CB[7]	CB[8]
outer diameter (Å)	a	13.1	14.4	16.0	17.5
cavity (Å)	b	4.4	5.8	7.3	8.8
	c	2.4	3.9	5.4	6.9
height (Å)	d	9.1	9.1	9.1	9.1
cavity volume (Å^3)	-	82	164	279	479

Fig. 1.10 | Structural Parameters for CB[n](n)5-8). Reproduced with permission.[16] Copyright 2003, ACS.

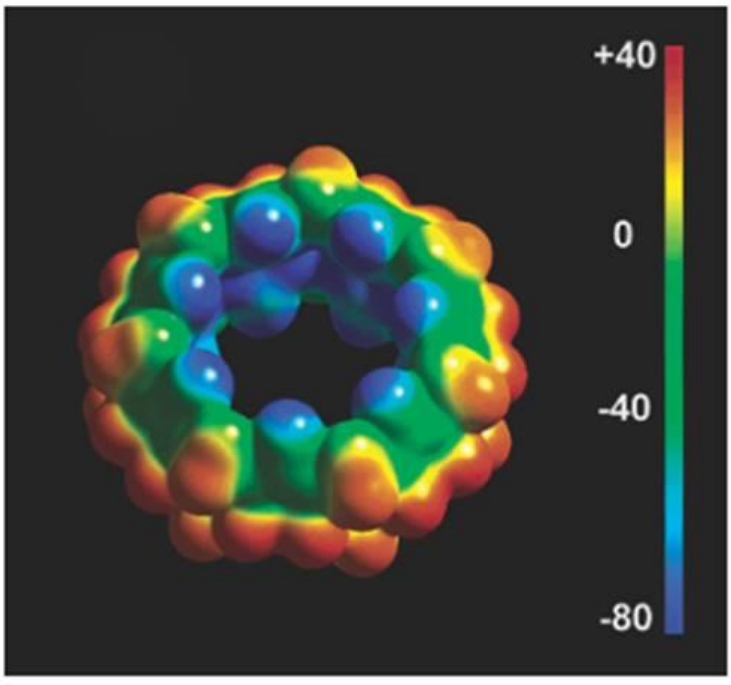

Fig. 1.11 | Electrostatic potential surfaces of CB[7]. Reproduced with permission.[16] Copyright 2003, ACS.

Electrostatic potential of surface of CB[n] gives ideas about nature of binding.[16] In CBs the regions around carbonyl oxygen's are found to be significantly negative (blue coloured) as expected.[16] The important thing to note that the inner surface of the cavity is also quite negative while the outer surface is somewhat positive (Fig. 1.11).[16] The covalent rigidity of CB[n] and dipolar nature of carbonyl portals both give the rich hydrogen-bonding ability and ion-dipole interactions contribute to the chemistry of these compounds.[15] The ion-dipole interactions are demonstrated by the fact that small cations which are bound in the carbonyllined portals are essential for solubilizing CB[6] in water. [15] The hydrophobic cavity of CB[n] favours encapsulation of neutral organic moieties due to favourable hydrophobic interaction.[14] These two binding environments of CB[n] have important implications on the guest exchange mechanism.[14] The carbonyl-lined portals can interact with monocations (like ammonium group) creating a series of encapsulation process for cationic guests.[15] The net encapsulation process required can be two type either occur by direct guest inclusion or by a stepwise process where the cationic moiety first binds to one of the carbonyl portals, followed by reorientation of the guest to allow for guest inclusion.[15] In case of monocationic guests, the organic portion of guest lies within the hydrophobic cavity, and the cationic portion interact with one of the portals.[15] For guests like pendent monocation, the monocation always occupies one of the carbonyl-lined

portals.[15] Overall guest inclusion process is in equilibrium, where CB[6] is in equilibrium with the 1:1 and 1:2 monocationic complexes (Fig. 1.12).[15]

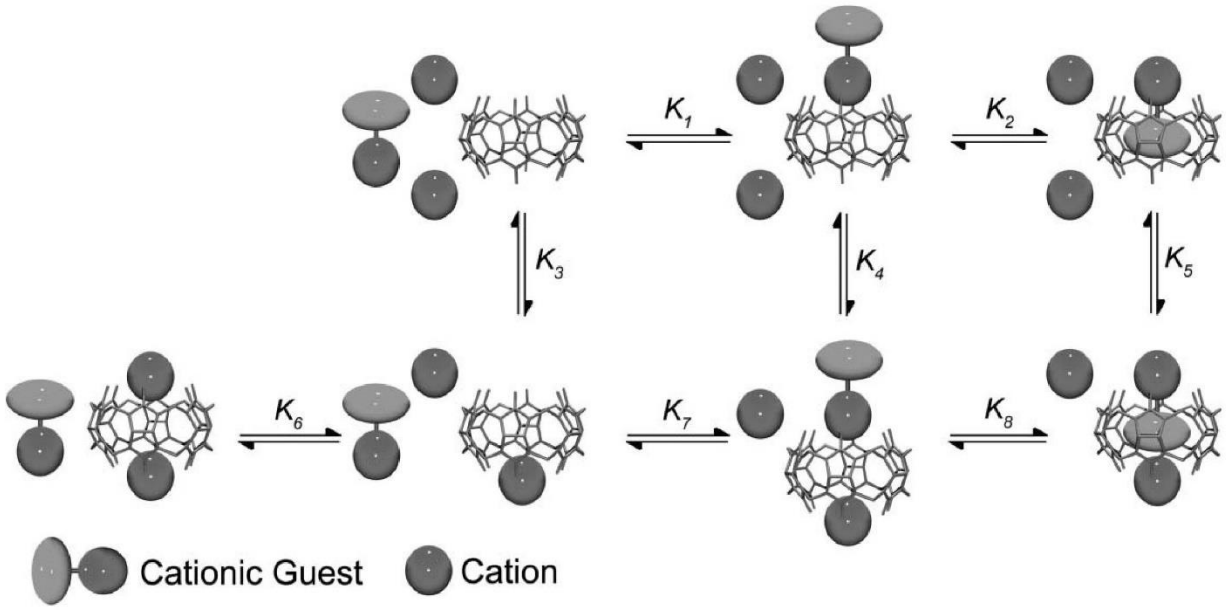

Fig. 1.12 | Complexation mechanism of mono cationic ammonium guest with Cucubit[6]uril. Reproduced with permission.[15] Copyright 2007, RSC

1.4 Stimuli-responsive based on the host-guest interaction of CB[7] and ADA

The guest binding affinity and selectivity of CB[7] are higher than those of any other synthetic receptors reported to date.[19] These nature of high affinity pairs offer numerous advantages including an attomolar dissociation constant and tunable complexation kinetics over other conventional macrocycles.[13] CB[7] shows remarkable binding characteristics based on the guest size, shape, length, and chemical functionalities.[17] The ultrastable host-guest complexes are unique as they rely on monovalent to achieve such high binding affinity.[18] The inherent high

affinity of CB[7] leads to the challenging applications in materials science, biology, and medicine.[19] Here are some vital examples of the application of the interaction of CB[7] and adamantylamine (ADA).

1.4.1 Host-guest interaction in drug delivery

Rotello and co-workers have utilized this bioorthogonal supramolecular interaction as a trigger mechanism in activation of nano therapeutics system.[20] Nano therapeutic system consists of gold nanoparticles functionalized with the diaminohexane terminal group and this nanoparticle form non toxic complex with CB[7] which is readily taken up by cells.[20] Removal of CB[7] from the nanoparticle surface using an orthogonal competitor guest ADA results in the endosomal escape of AuNP-NH_2, and cationic nanoparticle can interact with cell efficiently and thereby causes cell death (Fig. 1.13).[20] This terminal diaminohexane moiety renders cytotoxicity to the nanoparticle and serves as a guest unit for the formation of a supramolecular complex with CB[7].[20] This example demonstrates this host-guest system interaction as a mechanism for the regulation of therapeutics that can function inside a living cell.[20]

1.4.2 Host-guest interaction in the regulation of enzyme activity

CB[7] has very high selectivity and high binding affinity towards selected guest molecules which is comparable to those natural non bonding interaction typically found in the interaction of proteins and antibodies toward their ligands.[21]

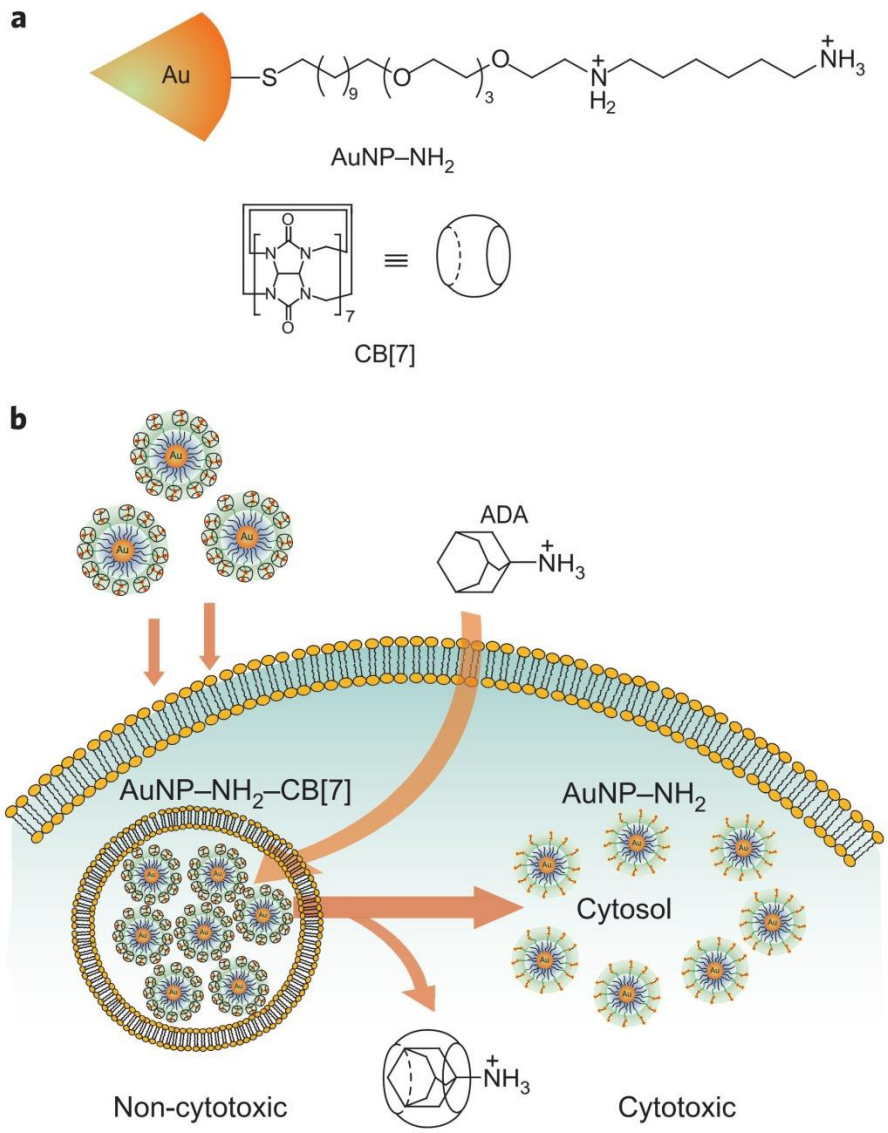

Fig. 1.13 | Schematic illustration of the use of host-guest complexation to trigger gold nanoparticle cytotoxicity. a) Structure of a diaminohexane-terminated gold nanoparticle ($AuNP–NH_2$) and CB[7]. b) Intracellular activation of $AuNP–NH_2$–

CB[7] cytotoxicity by removing of CB[7] from the nanoparticle surface by ADA. Reproduced with permission.[20] Copyright 2010, Nature Publishing Group.

Isaacs and co-workers developed a allosteric regulation mechanism based on CB[7], and ADA functionalized receptor work similarly to biological receptors and thereby changed in their biological activity (fig. 1.14).[21] They regulated the catalytic activity of BCA, with the help of a two-faced guest, which can bind to CB[7] in one face and to enzyme on another face.[21] The active site of the enzyme was initially occupied by a two-faced inhibitor that contains benzenesulfonamide(enzyme inhibitor unit) and trimethylsilylmethyl-ammonium group (CB[7] binding unit).[21] The initial enzymatic activity was restored by the addition of CB[7], which forms a 1:1 host-guest complex with trimethylsilyl-methylammonium part (Ka $\sim 10^9$ M^{-1}) of the two-faced guests to release the inhibitor from the enzyme.[21] However, the enzyme activity was inhibited again by the addition of adamantaneammonium derivative, which triggered the dissociation of the CB[7]-enzyme inhibitor resulting in the release of the free two-faced guest, which then re-occupied the catalytic site of the enzyme.[21] One of the key controlling factors in this process is the relative binding affinity of the two-faced inhibitors toward enzyme versus CB[7].[21] The exciting aspect is the ability of CB[7] to enhance the rate of dissociation of the enzyme- inhibitor by the transient formation of the enzyme-inhibitor CB[7] ternary complexes.[21] Strategy

differs from the typical allosteric regulation of enzyme activity, in that direct competition between two receptors (enzyme and CB[7]) is involved.[21] This finding demonstrates the advantage of CB[7] selectivity towards specific guest molecules, and hence it may be possible to use this receptor to control the activity of specific portions of the biological interaction networks.[21]

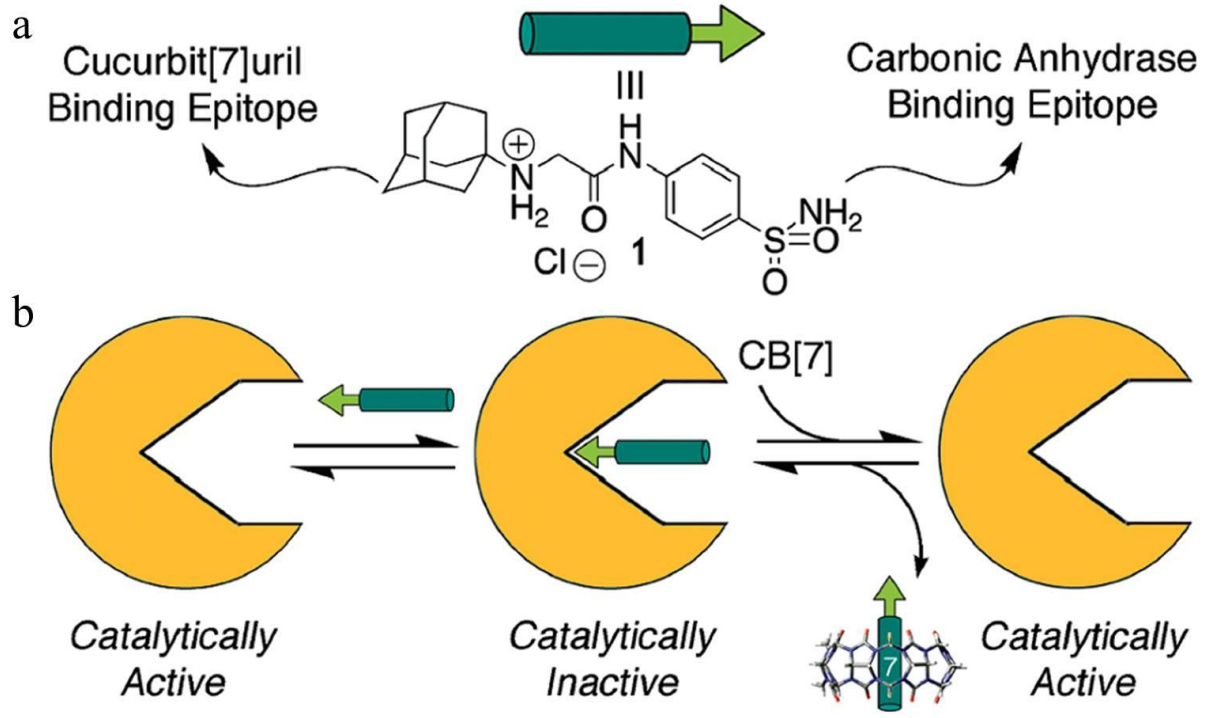

Fig. 1.14 | **a)** Structure of ADA derivative with CB[7] binding sites and BCA binding sites. **b)** Schematic illustration of the control of enzymatic activity using CB[7] and an adamantaneammonium derivative in a reversible fashion. Reproduced with permission.[21] Copyright 2010, American Chemical Society.

1.4.3 Host-guest interaction in activation of artificial nano-zyme

Rotello and co-workers have explored the benefit of high-affinity CB[7]-ADA pairs for the regulation of bio orthogonal catalysis in cells.[22] They developed a nano-zyme through the encapsulation of hydrophobic transition metal catalysts into the hydrophobic part of ligand monolayer of water-soluble gold nanoparticles.[22] The activity of the catalyst was regulated by using CB[7] as the 'gate-keeper' onto the monolayer surface.[22] The nanozyme is made of 2 nm gold nanoparticle in diameter, which is functionalized with a monolayer of polyethylene glycol (PEG)-alkanethiols that having end functional group dimethylbenzylammonium (DMBA) group.[22] The lipophilicity of the alkyl moieties enables the encapsulation of hydrophobic organometallic catalysts in hydrophobic part of the monolayer, while the end DMBA groups act as guest for CB[7]. The addition of CB[7] leads to the formation of DMBA–CB[7] complexes on the outer periphery of the nanoparticle, which sterically block access of small molecules to the internal catalytic domains.[22] They demonstrate that such nano engineered devices can enter cervical cancer HeLa cells by endocytosis and remain in a catalytically inactive state until a specific triggering signal, the guest molecule ADA is added.[22] The ADA molecules displace the DMBA groups from the hosting pocket of the CB[7]. This removal of shielding (CB[7]) exposes the

internally captured catalysts, which are then able to start catalysis of artificial substrates to the desired product.[22]

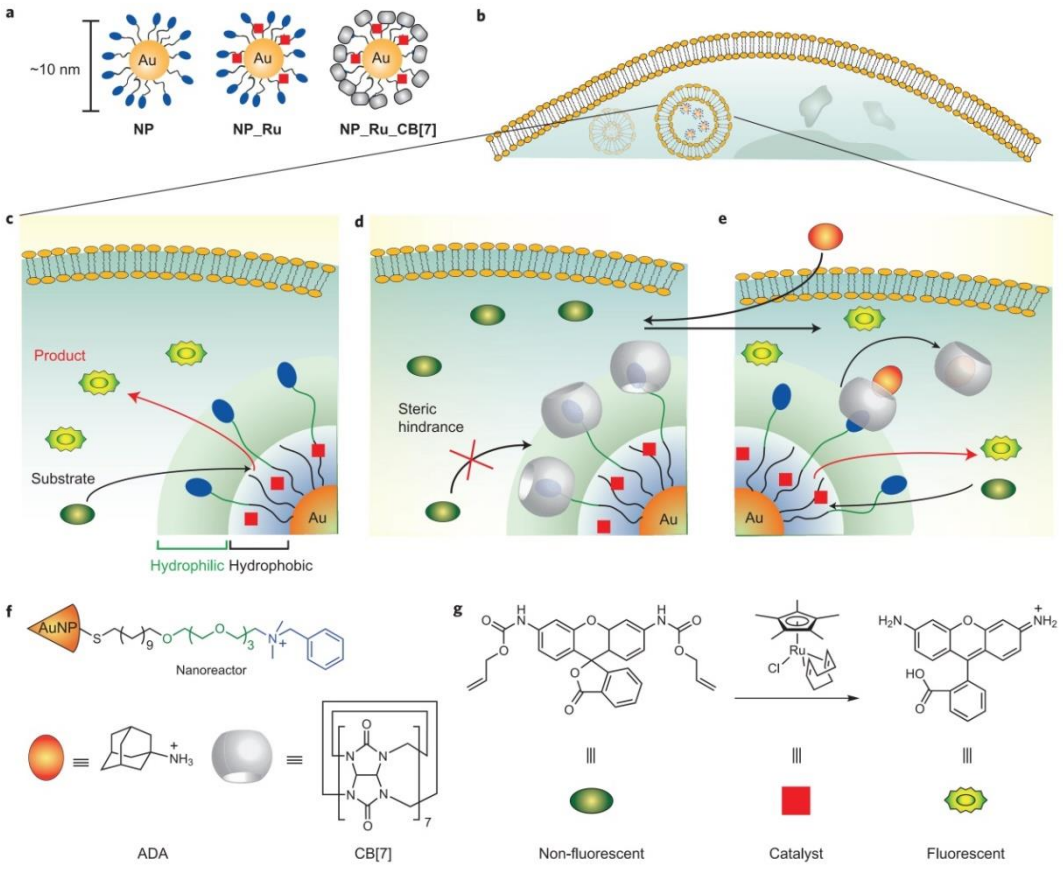

Fig. 1.15 | Artificial nanozyme design and activation of nanozyme intracellularly. **a)** AuNP, Ru-catalyst-embedded AuNP, and CB[7]-capped RU-catalyst-embedded AuNP. **b)** Cellular uptake of nanozymes. **c)** Catalysis substrate into the product by NP_Ru. **d)** Catalyst inhibition by capping of CB[7]. **e)** Regain of activity of nanozyme by removing CB[7] by ADA. **f)** Structures of the AuNP, CB[7] gatekeeper and ADA. **g)** Structures of the non-fluorescent substrate (rhodamine 110 derivative), fluorescent product (rhodamine 110) generated due to catalysis,

and Ru-catalyst for allylcarbamate cleavage. Reproduced with permission.[22] Copyright 2015, Nature Publishing Group.

1.5 Conclusion: From the respective example given here we can say that dynamic NP assembly and bioorthogonal supramolecular interaction of CB[7] and ADA both individually shows very good potential applications. Integrating the concept of two different system into a single system can lead the development of stimuli responsive, dynamic material, which can meet the demands of advanced drug delivery.

1.6 Present work

The thesis work is mainly focused on developing stimuli-responsive drug delivery system based on dynamic nanoparticle assembly system driven by bio-orthogonal supramolecular interaction, which will be discussed in chapter 2. Here dimethylbenzylamine functionalized gold nanoparticles was used as building block for generating dynamic assembly, where CB[7]⊣ADA host-guest chemistry serves as the fundamental mechanism. Our studies involve characterization and application of this nanoparticle assembles system as stimuli-responsive drug delivery system. Further, this assembly has been made responsive to light. This orthogonal light stimulus will be discussed in chapter 3.

References

1. Li, F., et al. Dynamic Nanoparticle Assemblies for Biomedical Applications. *Advanced Materials*. **2017**, *29*(14): 1605897.

2. Kundu, P. K., et al. Controlling the lifetimes of dynamic nanoparticle aggregates by spiropyran functionalization. *Nanoscale.* **2016**, *8*(46): 19280-19286.

3. Das, S., Dual-Responsive Nanoparticles and their Self-Assembly. *Adv. Mater.* **2013**, *25*, 422–426.

4. Verma, A., et al. Modulation of the Interparticle Spacing and Optical Behavior of Nanoparticle Ensembles Using a Single Protein Spacer. *Chemistry of Materials.* **2005**, *17*(25): 6317-6322.

5. Manna, D., et al. Orthogonal Light-Induced Self-Assembly of Nanoparticles using Differently Substituted Azobenzenes. *Angewandte Chemie International Edition.* **2015**, *54*(42): 12394-12397.

6. Wang, L., et al. Dynamic Nanoparticle Assemblies. *Accounts of Chemical Research.* **2012**, *45*(11): 1916-1926.

7. Samanta, D. and R. Klajn. Aqueous Light-Controlled Self-Assembly of Nanoparticles. *Advanced Optical Materials*. **2016**, *4*(9): 1373-1377.

8. Euan R. Kay., dynamic covalent Nanoparticle Building Blocks. *Chem. Eur.J.* **2016**, *22*, 10706 –10716.

9. Kundu, P. K., et al. Light-controlled self-assembly of non-photoresponsive nanoparticles. *Nature Chemistry*. **2015**, *7*: 646.

10. Zhao, H., et al. Reversible trapping and reaction acceleration within dynamically self-assembling nanoflasks. *Nat Nano*. **2016**, *11*(1): 82-88.

11. Kim, Y., et al. Transmutable nanoparticles with reconfigurable surface ligands." *Science.* **2016**, *351*(6273): 579-582.

12. Ohta, S., et al. DNA-controlled dynamic colloidal nanoparticle systems for mediating cellular interaction. *Science.* **2016**, *351*(6275): 841-845.

13. Barrow, J. S., Cucurbituril-Based Molecular Recognition. *Chem. Rev*. **2015**, *115*, 12320−12406.

14. Nau, M. W., Mechanism of Host-Guest Complexation by Cucurbituril. *Journal of the American Chemical Society,* **2004**, *126*, 5806-5816.

15. Pluth, D. M., Reversible guest exchange mechanisms in supramolecular host–guest assemblies. *Chem. Soc. Rev*. **2007**, *36*, 161–171.

16. KIM, K., Cucurbituril Homologues and Derivatives: New Opportunities in Supramolecular Chemistry. Accounts of Chemical Research, **2003**, 36(8), 621-630.

17. Mock, W. L. and N. Y. Shih. Structure and selectivity in host-guest complexes of cucurbituril. *The Journal of Organic Chemistry.* **1986**, *51*(23): 4440-4446.

18. Masson, E., et al. Cucurbituril chemistry: a tale of supramolecular success. *RSC Advances.* **2012**, *2*(4): 1213-1247.

19. Ma, X., Biomedical Applications of Supramolecular Systems Based on Host−Guest Interactions. *Chem. Rev*. **2015**, *115*, 7794−7839.

20. Kim, C., et al. Recognition-mediated activation of therapeutic gold nanoparticles inside living cells. *Nature Chemistry.* **2010**, *2*: 962.

21. Ghosh, S. and L. Isaacs. Biological Catalysis Regulated by Cucurbit[7]uril Molecular Containers. *Journal of the American Chemical Society*. **2010**, *132*(12): 4445-4454.

22. Tonga, G. Y., et al. Supramolecular regulation of bioorthogonal catalysis in cells using nanoparticle-embedded transition metal catalysts. *Nature Chemistry*. **2015**, *7*: 597.

Chapter2: Supramolecularly triggered release of therapeutics from dynamic nanoparticle assembly.

2.1 Introduction

Stimuli responsive devices that deliver a drug in spatial-, temporal- and dosage-controlled fashions can overcome the problem of systematic toxicity.[1,2,3,4] Implementation of such devices requires the use of materials that are susceptible to a specific physical incitement or that, in response to a specific stimulus.[5] Stimuli-responsive systems that can control drug biodistribution in response to specific stimuli, either exogenous (variations in temperature, magnetic field, ultrasound intensity, light or electric pulses) or endogenous(changes in pH, enzyme concentration or redox gradients) can meet the demand of advanced drug delivery.[5] Stimuli responsive drug delivery system based on exogenous and endogenous stimuli shows promising advantages over conventional drug delivery system, but these stimuli responsive drug delivery systems is not applicable in deep tissues.[6] All kind of exogenous stimuli cannot penetrate very deep into the tissues and not able to show desired stimulated effect.[6] However, small molecules can easily penetrate into the body in any sites; so stimuli responsive drug delivery system based on the small molecules can overcome this limitation.[6]

Nanoparticles are a promising candidate for drug delivery because of its different exciting property like surface plasmon, photothermal effect, easy surface decoration, etc.[7] Different stimuli responsive dynamic nanoparticle assembly has been developed widely with the aid of different stimuli other than small molecule

and system demonstrated mostly in organic solvents.[8] Development of stimuli responsive, dynamic nanoparticle assembly based on small molecular interaction which can work in water medium can lead essential applications.[8] Bioorthogonal supramolecular interaction of cucurbit[7]uril (CB[7]) and *adamantylamine* (ADA) is biocompatible and shows effectiveness inside living cell, so provides an excellent starting point for the development of dynamic nanoparticle assembly guided by this supramolecular interaction.[11,12]

Here in this present chapter, we developed simple approach of making a small molecule (as stimuli) responsive drug delivery system based on dynamic nanoparticle assembly by exploiting reversible nature of supramolecular interactions between functionalized gold nanoparticles (AuNPs) and CB[7]. AuNPs functionalized with dimethylbenzylamine (AuBz) group were used for the present studies. AuBz's by design is water soluble due to the presence of tetra (ethylene glycol) (TEG) unit and the cationic charge and the terminal functional group dimethylbenzylamine moiety act as a specific guest to CB[7]. As the interaction is supramolecular, so due to the inherent reversibility of supramolecular interaction system we can alter the interaction by another competitive guest to disassemble the CB[7] mediated assembly. This self-assembled AuBzs were treated with ADA which is known to have a very high association constant with CB[7] (Ka= $1.7X10^{12}$), whereas binding constant between benzyl ligand on NP and

CB[7] is K_a=1.6±0.32 $X10^5$ M^{-1} , thus leading the particle to disassemble.[13] We have seen that an amount of ADA equivalent to the total CB[7] in the assembled state, can disrupt the assembly through competitive binding. Experiments carried out in this direction resulted in disassembly and generated the initial nanoparticle (Fig 2.1). As during formation of this assembly, there will be generation of void space inside the construction and this can be effectively utilized to trap the drug molecules. So this process can be utilized for loading of drugs and small molecules in assembly and can be delivered at a later time point. This dynamic nanoparticle assembly has been shown to encapsulate *doxorubicin* (DOX), *camptothecin* (CPT) and their triggered release by small molecule stimuli, ADA. Finally, this stimuli responsive triggered release from the dynamic nanoparticle assembly was demonstrated through cell culture studies.

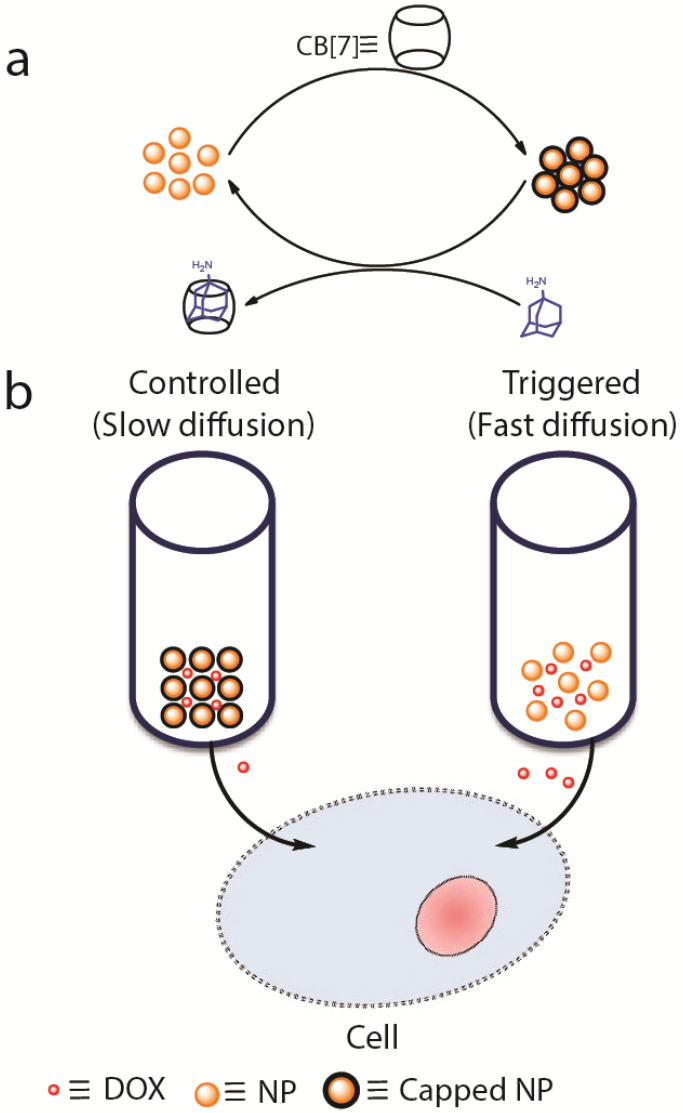

Fig 2.1 | Dynamic nanoparticle assembly and design of stimuli responsive supramolecular drug reservoir (SDR). a) Reversible assembly of functionalized nanoparticles(AuBz) driven by CB[7] and disassembly of nanoparticles by ADA by host-guest complexation. **b)** Controlled release of drug molecules from SDR due to slow diffusion of drug molecules and triggered release by ADA due to rupture of SDR.

2.2 Results and discussion

2.2.1 CB[7] mediated AuBz nanoparticle assembly

Initially, AuBz was mixed with CB[7] soln to test whether this nanoparticle undergo any assembly or not. When 6 nm AuBzs nanoparticle was mixed with CB[7] in the ratio of C_{NP}:$C_{CB[7]}$=1:3000, nanoparticle formed the assembly instantaneously and the supernatant became colourless. As shown in Fig 2.2, when CB[7] was added to the nanoparticle solution, the red solution turned colourless as all nanoparticle aggregated and precipitated from the solution. The morphological characterization of nanoparticle assembly was performed by TEM showing aggregates of nanoparticles (Fig 2.2b). However, Fig 2.2a shows well dispersed nanoparticles having same concentration. Since AuBz is polar, it is water soluble. When CB[7] capped the cationic ammonium group on the nanoparticle surface, the cationic charge gets shielded from the water molecule. As water molecule cannot interact with the nanoparticle, it starts getting aggregated with each other and finally gets precipitated.

2.2.2 Reversible assembly of gold nanoparticles

UV-vis spectra monitored the effect of CB[7] on the plasmonic absorbance of AuBz nanoparticles. The absorbance of gold nanoparticle depends on the number and proximity of other nanoparticles and also on the solvent in which it is dissolved. When CB[7] was added to the soln of AuBz nanoparticle, plasmonic

absorption maximum shows a red shift. On gradual addition of CB[7], the absorption maximum shifts from 525 nm to 534 nm and slowly the absorption spectra becomes wider (Fig 2.3). As CB[7] and ADA form supramolecular complex due to their inherent reversible nature , supramolecular interaction system will work reversibly on alternative addition. On addition of CB[7] in the ratio of C_{NP}:$C_{CB[7]}$=1:600 plasmonic maximum of NP shifts from 525 nm to 534 nm, further addition of ADA in the same ratio brings the plasmonic absorption maximum again to 525 nm. This reversible transition of plasmonic absorbance happens multiple times on sequential addition of CB[7] and ADA.

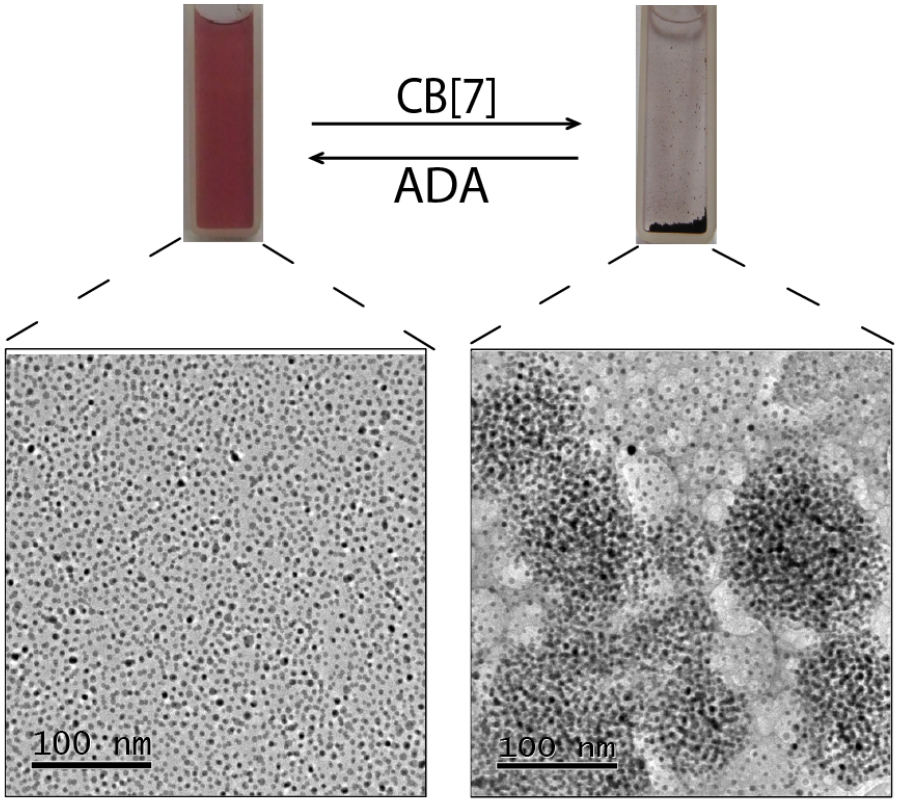

Fig 2.2 | TEM images of the dispersed (left) and aggregated (right) AuBz NPs.

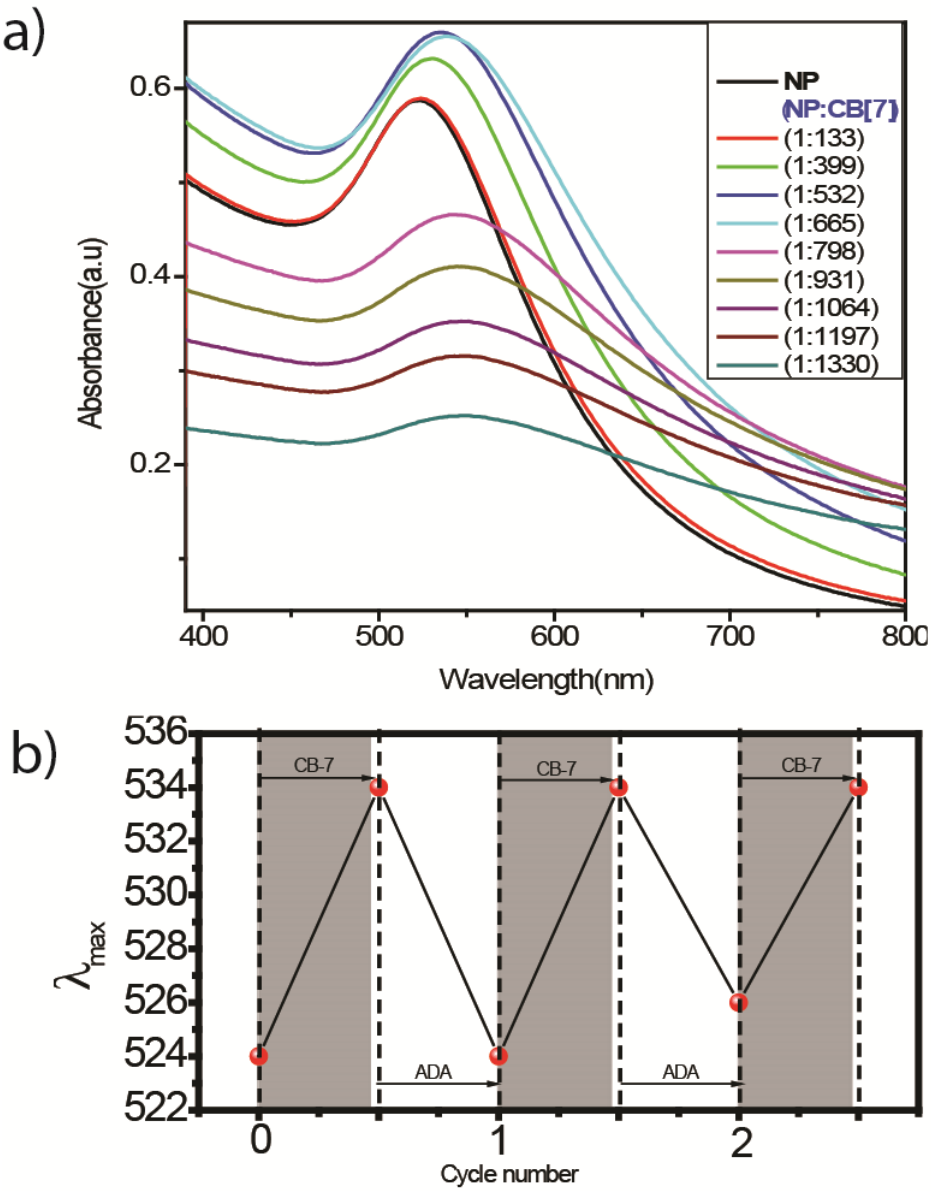

Fig 2.3 | Reversible NPs assembly driven by supramolecular interaction between CB[7], AuBz NP, ADA. **a)** A series of UV-vis spectra that accompanied with the nanoparticle aggregation on the gradual addition of CB[7]. **b)** Reversible changes in absorption maximum by alternative addition of CB[7] and ADA.

2.2.3 Encapsulation of therapeutics in dynamic nanoparticle assembly

To study the encapsulation efficiency inside the SDR during assembly formation, fluorophore conjugated protein (BSA-FITC), DNA (16nt-DNA-Atto) and drug (Doxorubicin) was encapsulated, simultaneously. In a solution of 6 nm AuBz nanoparticle all the three molecules were given in the ratio of C_{NP}:C_{DOX}=1:12.5, C_{NP}:$C_{DNA\text{-}Atto}$ =1:0.5, C_{NP}:$C_{BSA\text{-}FITC}$ =1:0.5 and then assembly was made by adding CB[7] (C_{NP}:$C_{CB[7]}$ =1:3000) to this mixture. Initially, fluorescence measurement of the fluorophore conjugated protein (BSA-FITC), DNA (16nt-DNA-Atto) and drug (Doxorubicin) was performed followed by the fluorescence measurement of the supernatant after assembly formation to understand the encapsulation efficiency. Fluorescence intensity dropped for all the three molecules after assembly formation which proves the encapsulation of molecules during dynamic assembly formation (Fig 2.4).

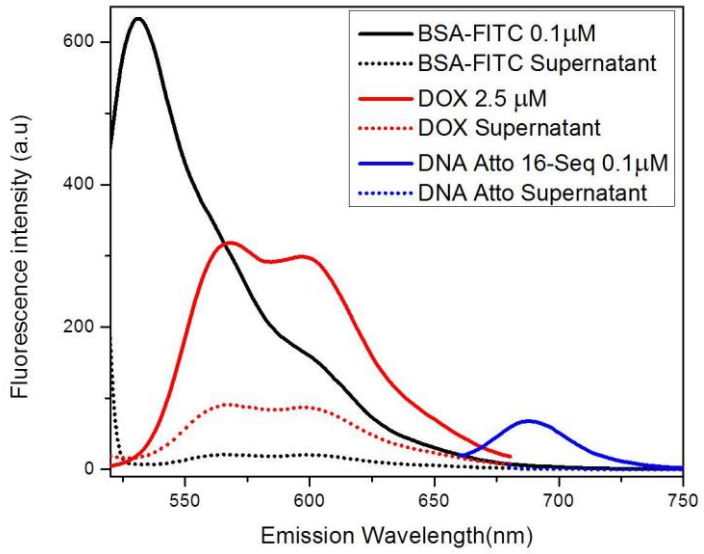

Fig 2.4 | Simultaneous encapsulation of therapeutics in AuBz assembly. Encapsulation of BSA-FITC, DOX, 16nt-DNA-Atto during assembly formation.

2.2.4 Encapsulation of active enzyme and catalysis

As the system has the capability to encapsulate drug, DNA and protein molecules, getting inspired by this result we attempted further to understand whether the system can encapsulate the enzyme in active and functional state. For a visual demonstration of enzyme encapsulation and catalysis of encapsulated enzyme, at first β-galactosidase was added in AuBz nanoparticle solution and assembly was made. The supernatant was removed, and the precipitate was washed with phosphate buffer saline (PBS) followed by the addition of fresh β- galactose solution into the assembly. Then we looked at the enzyme activity of the assembly in PBS medium on β-galactose which is sensitive to β-galctosidase. After few

minutes, the clear solution turns to yellow confirming that enzyme is trapped in the assembly which is responsible for catalysis. The time required for the cleavage of β-galactose to nitrophenol was noted by a change in colour from colourless to yellow (Fig 2.5) as well the encapsulated enzyme can catalyze the substrate in multiple cycles (Fig 2.6). After first catalysis, the supernatant was removed and assembly was treated with fresh β-galactose solution and again similar colour change was observed after a certain time interval. This result proves that this system could be effectively used for the controlled activity of enzyme over an extended period at the site of its action.

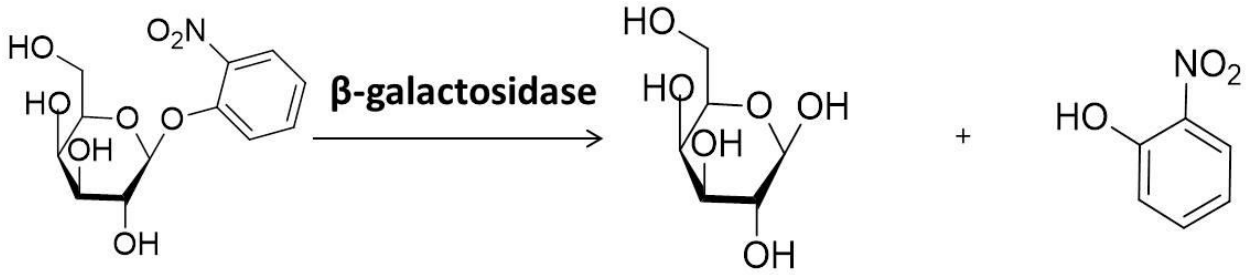

Fig 2.5 | Cleavage of β-galactose by β –galactosidase. Nitrophenol generates on cleavage responsible for the colour change.

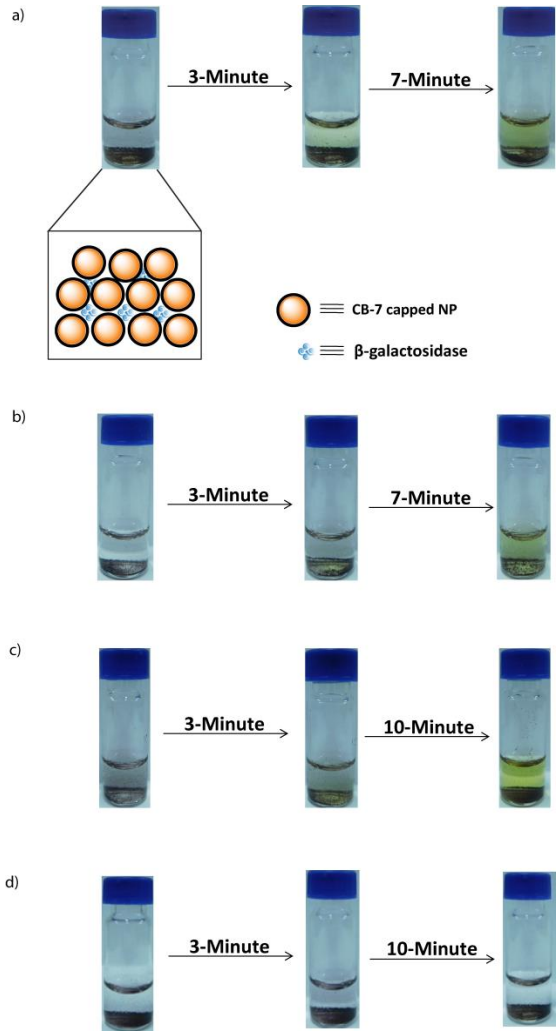

Fig 2.6 | β-galactosidase encapsulation inside assembly and repetitive activity of the encapsulated enzyme on betaglactose. a) enzymatic cleavage of betaglactose by encapsulated at first cycle, **b)** Enzymatic cleavage at second cycle, **c)** Enzymatic cleavage at third cycle. **d)** Control experiment assembly not containing encapsulated enzyme, so catalysis does not happen, and no color change observed.

2.2.5 ADA triggered DOX release

Control and stimuli enhanced release of drug molecules from SDR were tested using DOX as model drug molecule. For this drug release experiment, an implant was made by pipette tips and polystyrene membrane inside which the drug encapsulated nanoparticle assembly was added. The implant was then placed inside the wells of a 24-well plate. For experimental purpose, two different assemblies were made, one contain DOX molecule (C_{NP}:C_{ADA}=1:300) while another without any drug molecule. After assembly formation by CB[7], the solution was centrifuged and the supernatant was removed. The assembly was then transferred into the implant which was placed inside the wells of 24-well plate. It was made sure that the lower part of the implant having the assembly was dipped into the media below to allow diffusion to happen. Fluorescence measurement was then performed. For the triggered set, ADA was added inside the implant in the ratio of ($C_{CB[7]}$: C_{ADA}= 1:1) at the 0 min time point of release kinetics. A clear enhancement of fluorescence intensity was observed at 60 min time point for the triggered set (Fig 2.7). The result below highlights the triggered release of DOX by ADA.

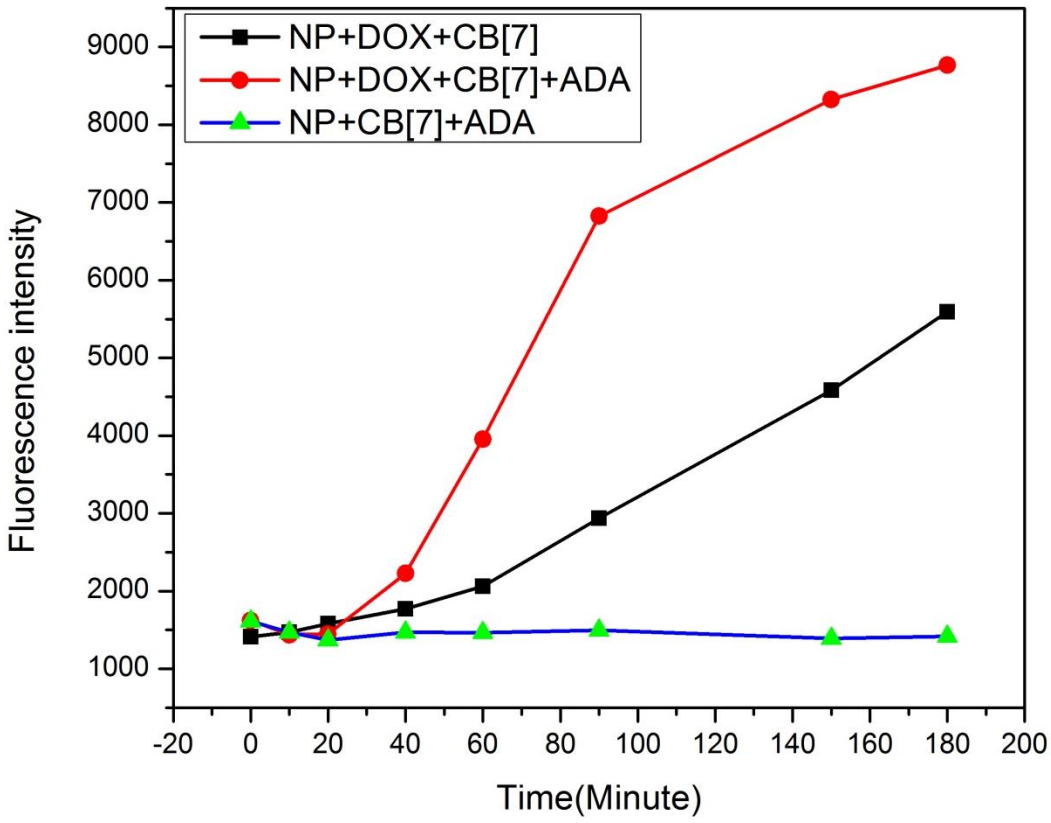

Fig 2.7 | Triggered release of Doxorubicin from SDR. Comparison of the drug release profile from SDR in a controlled set (black line) and triggered by ADA (red line), C_{NP}:C_{DOX}=1:300, C_{NP}:C_{ADA}=1:3000.

2.2.6 Extended release of camptothecin

It was observed from the earlier study that the release of DOX from the assembly was very fast, the process was completed by 200 minutes. For practical application, the release of drug should be released for long time of duration from the drug delivery system. To establish a long-lasting release profile, we alter the drug

molecule to CPT, another anticancer drug molecule. When release profile from the assembly of nanoparticle was studied, we observe a long duration of release of CPT from the assembly (Fig 2.8). This experiment shows how the drug molecule release profile from the assembly depends on the drug molecules.

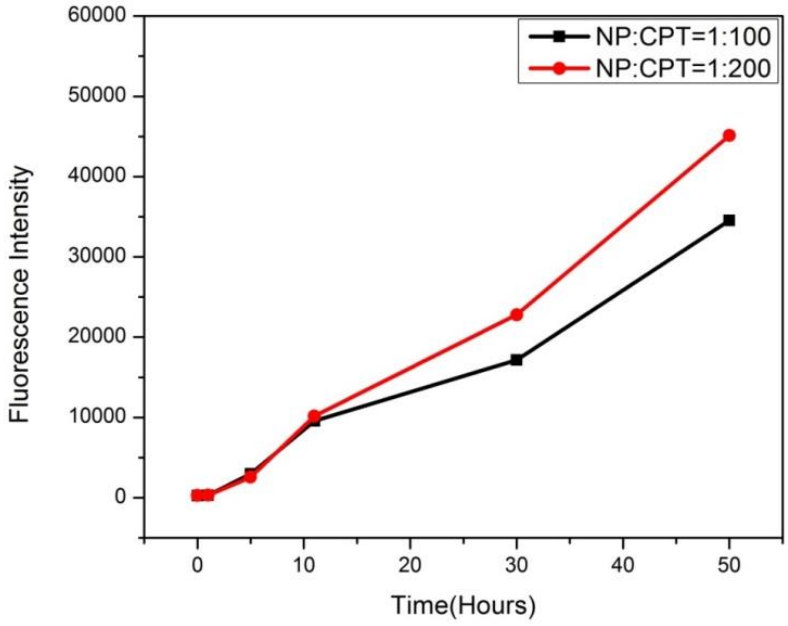

Fig 2.8 | Extended release of Camptothecin (CPT) from the SDR in two different conditions.

2.2.7 ADA triggered enhanced cytotoxicity of DOX

To validate our drug release from SDR in the cells, Hela cells (human cervical cancer cell line) was chosen. The assembly was made as described earlier (section-2.2.6) and similarly was placed inside the 24-well cell culture plate using the implant having ~50,000 cells/1mL media. The triggered experiment was performed with ADA with amount $C_{CB[7]}$:C_{ADA}=1:1 and implant were removed from the cell culture plate after 90 minutes. The cells were then incubated for 24 hours at 37^0C. To obtain a visual understanding of the viability of the cell, bright field images of the cell were taken after 24 hours (Fig 2.10). From the images, it is clear that the cells are less viable where SDR is containing drug and is triggered by ADA. On the other hand, in the absence of drug, the triggering by ADA does not show any reasonable toxicity. The same result was also concluded from the cytotoxicity study by Alamar blue assay. Thus from here it can be proved that this enhanced cytotoxicity due to triggering by ADA was due to the increased amount of DOX released by the triggered effect.

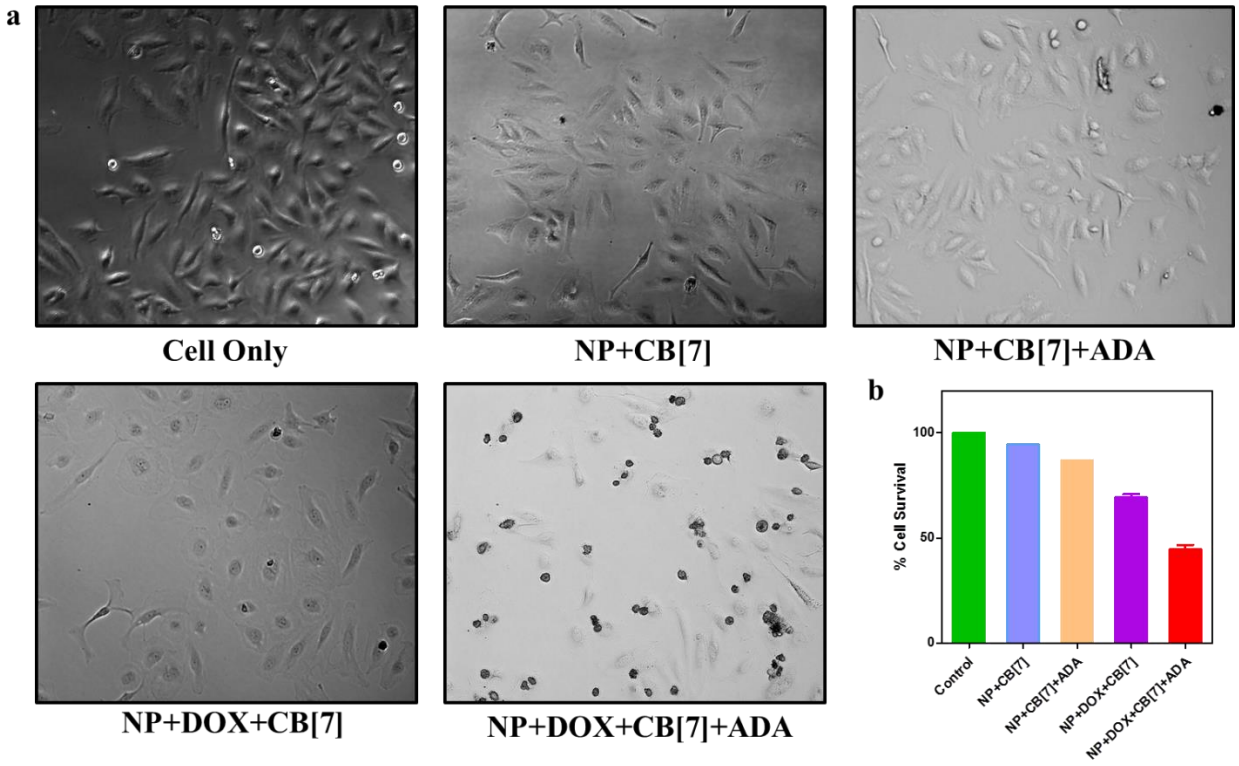

Fig 2.9 | Cytotoxicity of Doxorubicin released from an implant in the controlled and triggered release. a) Brightfield images of HeLa cells treated with SDR without DOX and SDR with DOX. The implant was removed after 90-minutes and cells were kept for 24-hours incubation at 37ºC. **b)** The viability of cells treated SDR with the drug, without the drug, triggered by ADA and only assembly triggered by ADA. SDR having encapsulated drug showing enhanced toxicity on ADA addition. SDR without encapsulated drug showing very low toxicity and even addition of ADA does not induce much toxicity.

2.2.8 Differential stimulant effect on cytotoxicity of SVEC cell

Cytotoxicity of DOX by the triggered release of ADA, showing differential trends depends on the amount of ADA used for stimulated release. Where the implants does not contain encapsulated DOX, there is no difference in cytotoxicity with different amount of ADA and thus cell viability remains almost unchanged (Fig 2.11). However, when the implants contain encapsulated DOX, cytotoxicity increases with the increasing amount of ADA, as clear from the right side of the (Fig 2.11). These results demonstrate that the amount of stimulant guide the release of the drug from the implant.

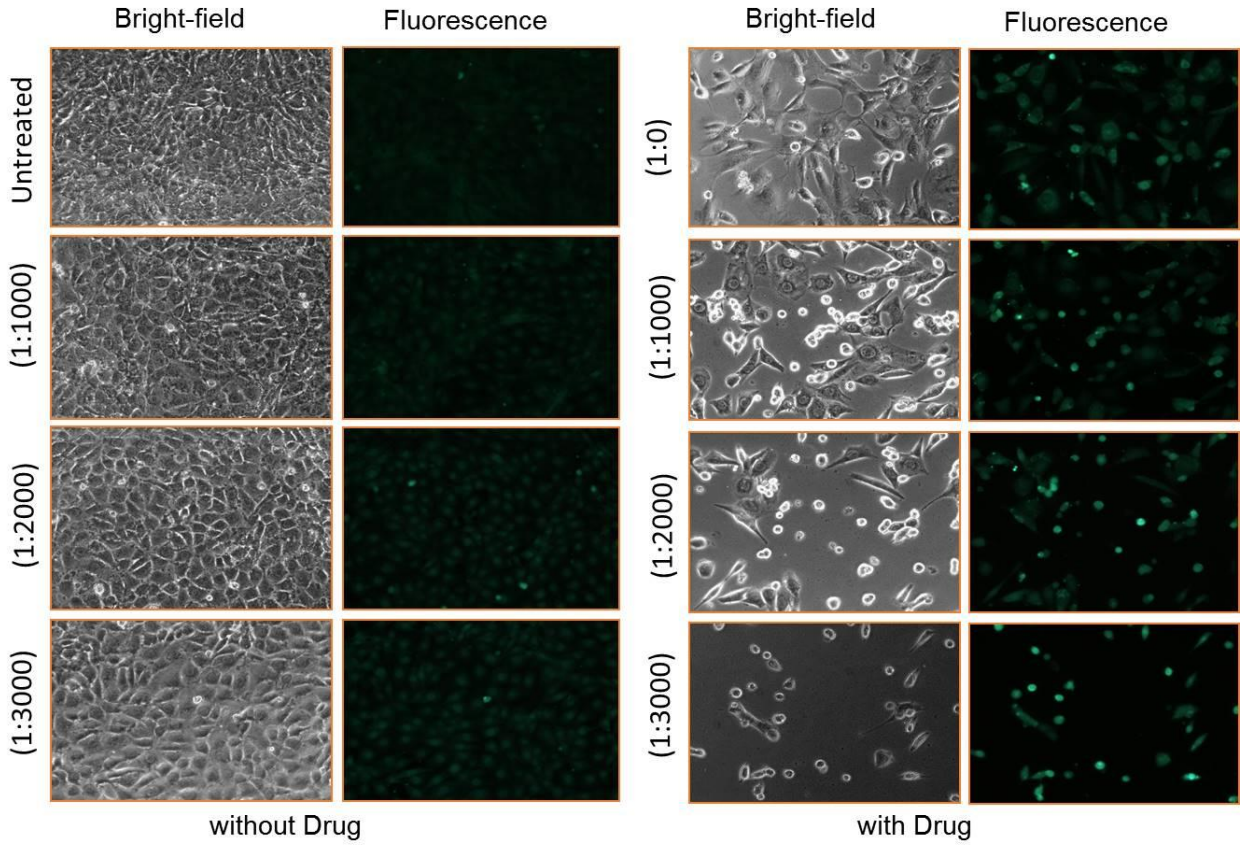

Fig 2.10 | Comparison of cytotoxicity possessed by controlled and triggered release. Depots without drug do not show any toxicity towards cells. Depots with encapsulated drug show higher toxicity with an increased amount of ADA. Cells were stained with calcein for visualisation by fluorescence.

2.3 Conclusion

In summary, we have presented here a simplistic way of small molecule-based stimuli responsive, dynamic nanoparticle assembly as controlled drug delivery system. Drug release profile can be enhanced by chemical stimuli have been demonstrated based on single nanoparticle system. Finally, our system has the capability of easy encapsulation of drug molecules and multiple therapeutics in its active and functional state without any chemical modification. Due to ease of fabrication and versatility, we envision that stimuli responsive, dynamic nanoparticle assembly directed by small molecule could play an extraordinary role in developing stimuli responsive drug delivery system.

2.4 Experimental section

2.4.1 Materials and methods

All the chemicals were purchased from Sigma Aldrich, Alfa Aesar or TCI India. Dichloromethane was dried according to the standard procedure. ^{1}HNMR spectra were recorded in Bruker AVANCE 400 FT-NMR spectrometer with chemical shifts reported in parts per million (ppm) with respect to Tetramethylsilane (TMS). Transmission electron microscopic (TEM) images were recorded on JEOL JEM-3010 operating at 300kV. Bright field images were acquired using a Zeiss Axio Vert A.1 inverted microscope.

2.4.2 Implant fabrication and setup

For the study of DOX release kinetics from SDR, an implant of cylindrical shape was made from the pipette tips and one cross-section of the implant was covered with nitrocellulose membrane (pore size 0.2 μm). First pipette tips were cut into two pieces, and the upper part of the tip was used for implant fabrication. The smooth outer part was heated in a flame and pressed on the top of the nitrocellulose membrane in the hot condition and pressed little so that it can stick to the membrane. The membrane was used to avoid transfer of assembly materials to the diffusing media (as nanoparticles create problem in fluorescence measurement) and allow only drug molecules to diffuse from the assembly to the media. For the

drug release and cell culture study, the membrane attached part of the implant was kept towards the bottom of 24-well plate using double sided tape in such a way that the implant hanged on the wall of 24-well plate and didn't touch the bottom surface of the plate. This finally facilitated diffusion of molecules smoothly from the assembly.

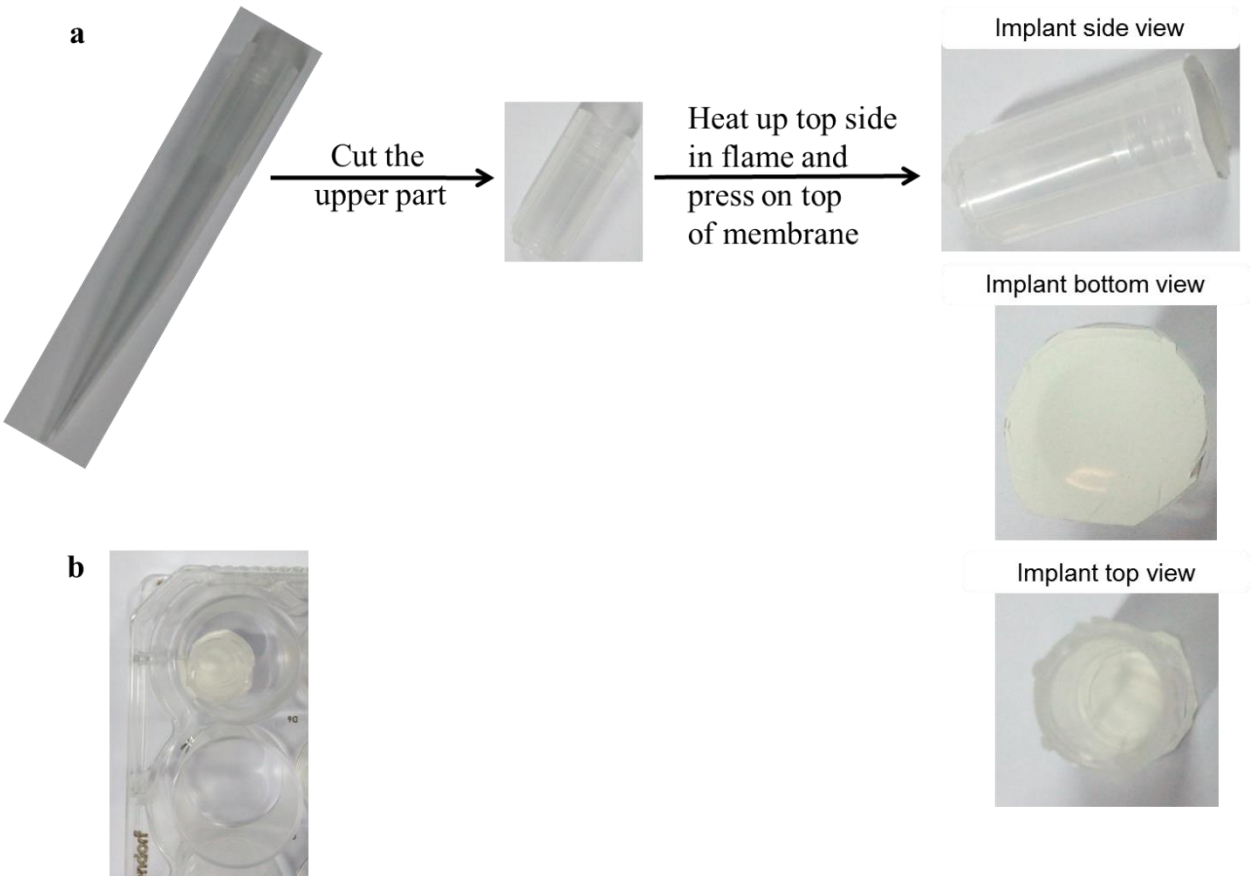

Fig 2.12 | Implant fabrication process used for drug release study and cell culture study. **a)** Fabrication of the implant from 1ml pipette tips through the represented way. **b)** Picture of implant placed inside the well of a 24-well plate.

2.4.3 4 nm undecanthiol gold np synthesis

In a round bottom flask, 100 mg gold(III) chloride trihydrate was dissolved in 50 ml deionized water by vigorous stirring. Tetraoctylammonium bromide (TOAB) 267 mg in 50 ml toluene was then added to the gold salt solution. Then 54 µl undecanthiol was added to above mixture, and the two-phase mixture was stirred for 10 min. Following that, 93 mg $NaBH_4$ in 5 ml cold deionized water was added very quickly, and the soln was stirred vigorously for 5 hours. Toluene layer was collected and evaporated in a rotary evaporator, a minimum amount of toluene, ~ 5 ml was left in 250 ml round bottom flask. Then remaining toluene was transferred to a 25 ml round bottom flask and evaporated to dryness and kept in vacuum for 6 hours. After complete drying, a black layer was formed on the wall of the flask. Then this crude product in the 25 ml round bottom flask was heated using heating bath under nitrogen atmosphere. The temperature was increased with the rate of 10℃ in every 5 min and maitained for 30 min at 150℃. After heating, the product was allowed to cool to room temperature and then dissolved in 500 ml methanol. The solution was put into the freezer overnight to allow the gold colloids to precipitate and to remove excess undecanthiol and TOAB. Methanol was then removed by decanting and the precipitate containining the nanoparticles was dissolved in 5 ml toluene.[14]

2.4.4 TEM characterization of 4 nm undecanthiol capped gold Np

30 nm concentration of 4 nm undecanthiol capped nanoparticle in toluene solution was drop casted on TEM grid and then kept 24 hours for drying before imaging.

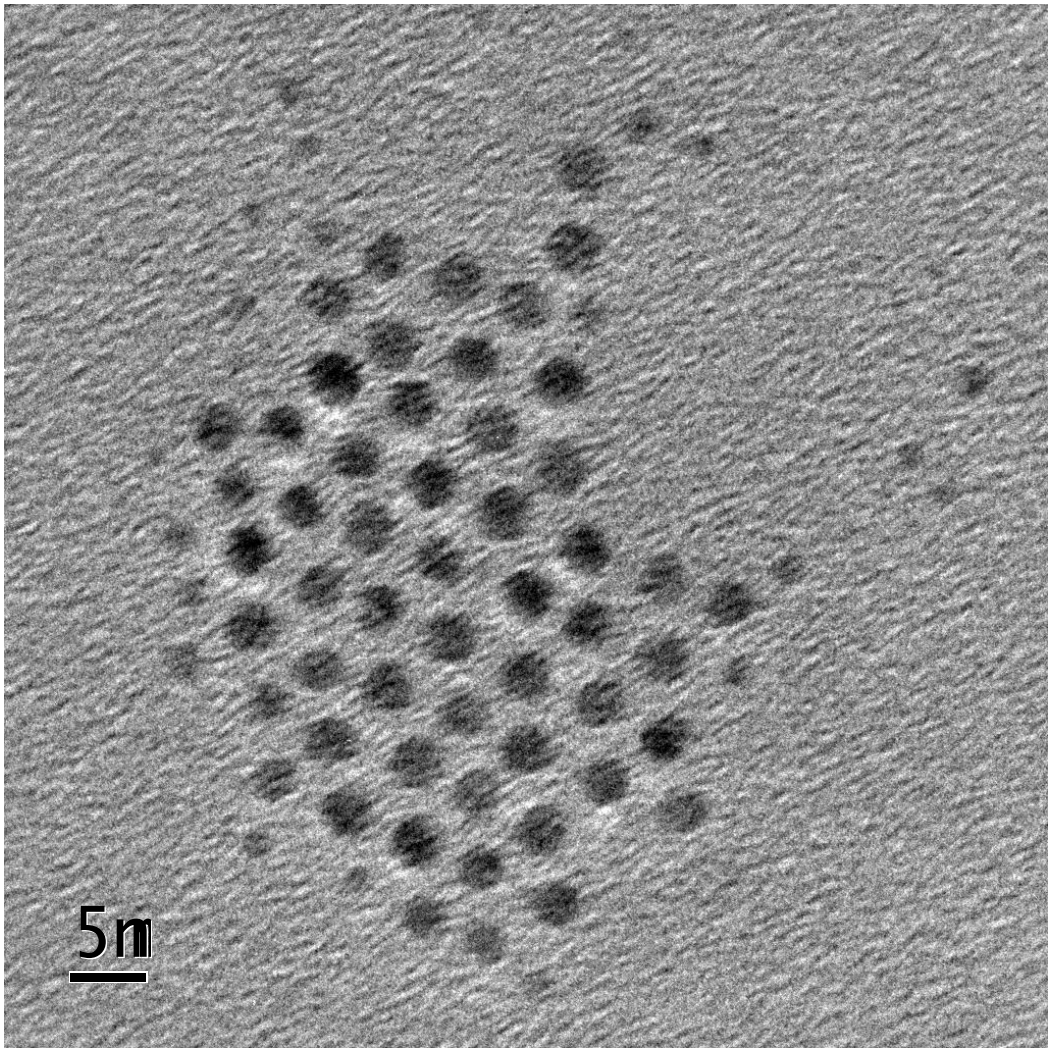

TEM images of undecanthiol capped gold nanoparticle of 4 nm average size.

2.4.5 Post functionalization of 4 nm nanoparticles

10 mg of undecanthiol thiol-capped AuNPs were dissolved in 2 ml of dry dichloromethane and purged with nitrogen. 50 mg of SH-C_{11}-TEG-NMe_2Bn thiolated ligands was dissolved in 2 ml of dry DCM and purged with nitrogen. Then solution of the thiolated ligand was mixed with the nanoparticle solution and kept under stirring for 48 hours. The solvent was then removed by rota evaporator, the nanoparticle was found dried and sticked to the glass vial surface. Then five-times washing with 5 ml of hexane was carried out to remove excess thiol ligands. After washing with hexane, the vial was kept open to dry up completely. Finally, the nanoparticle was dissolved in Milli-Q water and dialysed with Milli-Q water for 24 hours.

2.4.6 Structure of post functionalized nanoparticle

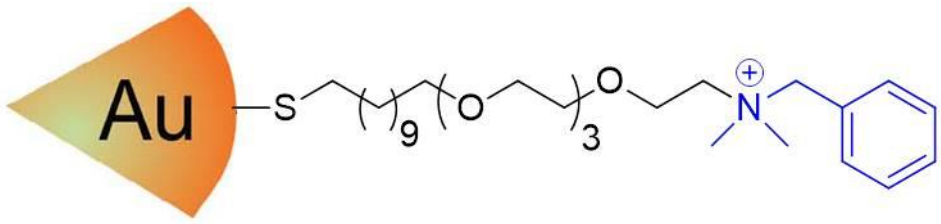

Structure of nanoparticle used for fabrication of SDR. Nanoparticle functionalized with dimethylbenzylamine group through a linker of HS-C_{11}-TEG. Here dimethylbenzylamine group work as a guest of CB[7].

2.4.7 TEM of 4 nm post functionalized nanoparticle

30 nM concentration of 4 nm post functionalized nanoparticle in water was drop casted on TEM grid and then kept in vacuum for 24 hours before imaging.

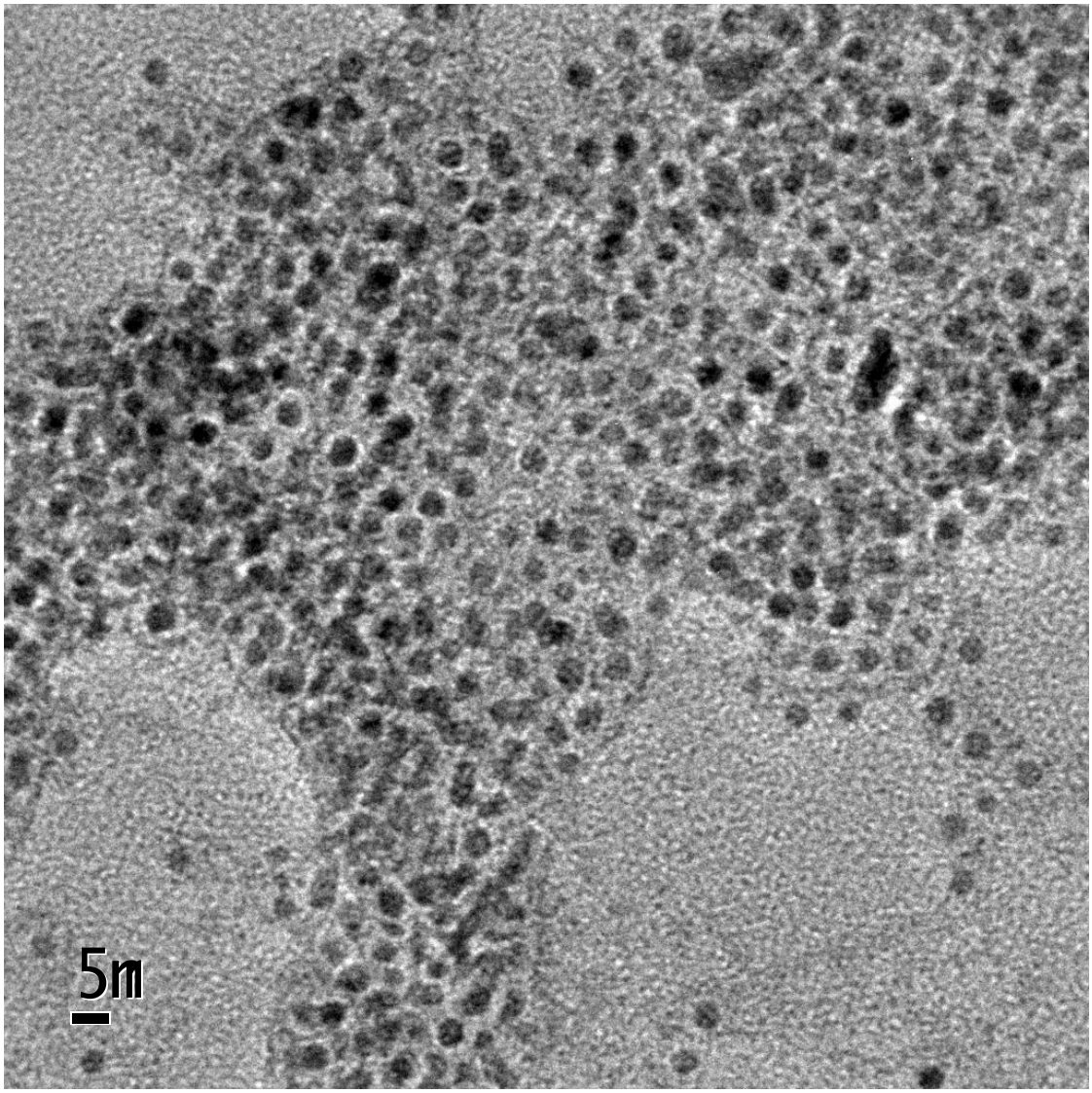

TEM images of post functionalized gold nanoparticle of 4 nm average size.

2.4.8 Sample preparation for TEM of 6 nm Post functionalized np assembly

6 nm benzyl nanoparticle soln of conc 30 nM was drop-casted on TEM grid and was kept for 24 hours in vacuum condition for drying. For assembly formation in 200 µl, 30 nM of 6 nm benzyl nanoparticle solution and 4.8 µl of 6 mM CB[7] soln was added [C_{NP}:$C_{CB[7]}$ =(1:4800)] and allowed to react for 5 minutes before drop-casting on TEM grid and then vacuum drying.

2.4.9 Reversibility of surface plasmon absorbance of gold nanoparticles

For studying the reversible plasmonic change of nanoparticle with sequential addition of CB[7] and ADA, 400 µl of 37 µM AuNP was taken in the cuvette. 4.44 µl of 2 mM CB[7] was added for making assembly, and after UV measurement 2 µl of 4.8 mM ADA was added to make the disassembly of the nanoparticle. For the consecutive cycle, the same amount of CB[7] and ADA was given into the solution in an alternative fashion.

2.4.10 Encapsulation of enzyme and catalysis

For a visual demonstration of enzyme encapsulation and catalysis of encapsulated enzyme, first β-galactosidase was added in the nanoparticle solution and the assembly was made. For experimental purpose, 550 µl of 0.1 µM of 6 nm benzyl

nanoparticle soln was taken and to that 30 µl of 500 nM β-galactosidase was added. The assembly was made by adding 9.16 µl of 15 mM CB[7] solution followed by centrifugation and removal of the supernatant without losing any assembly. Further assembly was washed with 100 µl PBS solution two times.Then 500 µl PBS was added to the assembly and freshly prepared 20 µl of 5 mM o-nitrophenyl β-galactoside was added, and the colour change was monitored over time. Multiple catalyses of the substrate were done removing supernatant from the assembly, washing once with 100 µl PBS and then again addition of 500 µl of PBS followed by the addition of same amount of substrate for further catalysis.

2.4.11 Assembly preparation for ADA triggered DOX release

In a 500 µl Eppendorf tube, 30 µl 5 µM 4 nm benzyl nanoparticle solution was taken and to that soln 18 µl of 2.5 mM DOX soln was added followed by the addition of 22.5 µl of 20 mM CB[7] to make the DOX encapsulated assembly. The ratio of the component used in the assembly formation was C_{NP}:C_{DOX}=1:300, C_{NP}:$C_{CB[7]=}$1:3000. After assembly formation,the mixture was centrifuged for 1 min at 50 rpm and the supernatant was removed without losing assembly. The assembly was then washed with 50 µl PBS soln and transferred by 50 µl media inside the implant (dipped into 1 ml phenol-red free media in 24 well plate). For the triggered release study, 22.5 µl of 20 mM ADA was added inside the implant, and the ratio of stimulant was C_{NP}:C_{ADA}=1:3000. Fluorescence measurement was performed in

a microplate reader (using Corning make flat-black 96-well plate) at different time points by taking 80 µl of media from the experimental well plate. The excitation and emission wavelengths for DOX were 480 nm and 570 nm respectively.

2.4.12 Assembly preparation for Hela cell culture study

Assembly was made in the same way as for point 6.

2.4.13 Hela Cell Culture

HeLa cells were used for the experimental study. The cells were cultured in a humidified atmosphere (5% CO_2) at 37°C and grown in Dulbecco's Modified Eagle's Medium (DMEM, high glucose) supplemented with 10% fetal bovine serum (FBS) (Gibco, USA), 2 mM Glutamax (Invitrogen, USA) and 1% antibiotics (100 U/ml penicillin, 100 µg/ml streptomycin and 0.25 µg/ml amphotericin) (Gibco, USA). Prior to experiment, the cells were seeded at ~50,000 cells/1000µL in a 24-well plate. After 24hrs, the cells were washed with 1X DPBS and implants were fixed in different wells and the assembly was added inside the implant. After 24 hrs, the cells were washed and incubated with media containing Alamar Blue solution (90µL media + 10µL 10X Alamar Blue per well) (as per standard protocol). After ~4hr incubation, the absorbance was measured at 570nm (experimental wavelength) and 600nm (reference wavelength) and the data was analysed.

2.4.14 Assembly preparation for CPT release study

For the CPT release study, two different assemblies were made where the ratio of NP and CPT were 1:100 and 1:200. In a 30 µl of 5 µm 4 nm Benzyl nanoparticle solution, 3 µl and 6 µl of 5 mM CPT was added the for making assemblies. Then 22.5 µl of 20 mM CB[7] soln was added and centrifuged for 1 min at 20 rpm followed by the removal of the supernatant. Assembly was transferred to the implant by 50 µl PBS. The implant was dipped in 1 ml of PBS solution. The release kinetics was studied in a microplate reader by taking 70 µl soln from the diffusing media.

2.4.15 SVEC Cell culture

Saphenous vein endothelial cell line (SVEC) was cultured in DMEM containing 10% FBS (Gibco-BRL, USA) and 2 mM Glutamax (Invitrogen, Carlsbad, USA). Cells were cultured in 24 well dish for 24 hours to 60% confluence before starting drug treatment. Drug treatments were performed by putting assembly and triggered agent inside the implant and continued for a period of 24 hours incubation and then washed twice in 1X Phosphate-Buffered Saline (PBS). There after, Calcein dye (Invitrogen, Carlsbad, USA) was added at a concentration of 5 µM and cells were incubated at 37 ˚C CO_2 incubator for an additional time of 30 minutes. Cells were washed twice in 1X PBS again and imaged in complete cell culture medium. Brightfield (phase contrast) or fluorescence images were captured with an inverted

fluorescence microscope (IX70, Olympus) using 10X or a 20X plan objective equipped with a cooled charge coupled device (CCD) camera (CoolSNAP; Roper Scientific, Inc).

2.4.16 Assembly preparation for the differential triggered release

In 43 µl of 3.7 µM nanoparticle solution, 5 µl of 0.8 mM DOX solution was added, then 140 µl CB[7] solution was further added for making the assembly. The solution was then centrifuged for 1 min at 50 rpm followed by the removal of the supernatant . The assembly was then transferred inside the implant using 100 µl media. For differential triggered effect, 13.2 µl, 26.4 µl, 39.6 µl of 12 mM ADA solution was added inside the implants where C_{NP}:C_{ADA} was 1:1000, 1:2000 and 1:3000 respectively.

References

1. Kearney, C. J. and D. J. Mooney. Macroscale delivery systems for molecular and cellular payloads. *Nat Mater*. **2013**, *12*(11), 1004-1017.

2. Park, K. Controlled drug delivery systems: past forward and future back. *J Control Release*. **2014**, *190*: 3-8.

3. Yun, Y. H., et al. Controlled Drug Delivery: Historical perspective for the next generation. *J Control Release*. **2015**, *219*: 2-7.

4. Park, K. Controlled drug delivery systems: past forward and future back. *J Control Release.* **2014**, 190: 3-8.

5. Mura, S., et al. Stimuli-responsive nanocarriers for drug delivery. *Nature Materials.* **2013**, *12*: 991.

6. Brudno, Y. and D. J. Mooney. On-demand drug delivery from local depots. Journal of Controlled Release. **2015**, *219*: 8-17.

7. Rotello,V. M., Gold nanoparticles in chemical and biological sensing. Chemical reviews, **2012**, *112* (5), 2739-2779.

8. Li, F., et al. Dynamic Nanoparticle Assemblies for Biomedical Applications. *Advanced Materials*. **2017**, *29*(14): 1605897.

9. Wang, L., et al. Dynamic Nanoparticle Assemblies. *Accounts of Chemical Research.* **2012**, *45*(11): 1916-1926.

10. Blum, A. P., et al. (2015). Stimuli-Responsive Nanomaterials for Biomedical Applications. *Journal of the American Chemical Society*. **2015**, *137*(6): 2140-2154.

11. Kim, C., et al. Recognition-mediated activation of therapeutic gold nanoparticles inside living cells. *Nature Chemistry*. **2010**, *2*: 962.

12. Tonga, G. Y., et al. Supramolecular regulation of bioorthogonal catalysis in cells using nanoparticle-embedded transition metal catalysts. *Nature Chemistry*. **2015**, *7*: 597.

13. Barrow, J. S., Cucurbituril-Based Molecular Recognition. *Chem. Rev*. **2015**, *115*, 12320−12406.

14. Teranishi, T., et al. (2001). Heat-Induced Size Evolution of Gold Nanoparticles in the Solid State. *Advanced Materials*. **2001**, *13*(22): 1699-1701.

Chapter 3: Light responsive dynamic nanoparticle assembly as stimuli responsive drug delivery system.

3.1 Introduction

Stimuli responsive drug delivery systems provide non invasive control of the availability of therapeutic molecules in living organisms.[1,2] Among all the external stimuli available, light has attracted particular attention due to its ease of production, noninvasive nature, controllable intensity, and spatially confined application for finely controlled durations. [3,4] Thus, light has been utilized in an abundance of applications for intelligent delivery systems that can provide good control of the treatment process and allow transport and release of drugs at disease sites.[5,6,7,8] Nanoparticles are an attractive system for drug delivery in different prospects due to their various exciting features.[9] Alternating the properties of materials in reversible fashion using external stimuli is an important concept for developing stimuli responsive materials.[10] Properties of self-assembly of nanoparticles (NPs) often depends on the degree of aggregation has attracted considerable attention due to its various interesting properties.[10] Several ways have been developed to reversibly assembling NPs in response to light, as this stimulus can be delivered remotely, with spatially confined and temporal precision, and in the form of different wavelengths.[11] An efficient way to make NPs responsive to light is based on functionalizing nanoparticle surfaces with monolayers of the photoswitchable trans-azobenzene, spiropyran molecules.[12,13] All this photosentive ligand functionalized NPs are mainly soluble in nonpolar

solvents. On exposure to UV light photoresponsive ligand undergoes a different transformation like cis-trans, cyclization; responsive to altering properties of nanoparticles.[14] In case of azobenzene functionalize NPs azobenzene isomerizing to the more polar cis-isomer, which induces attractive interparticle interactions, resulting metastable NPs aggregates, and they disintegrate in the dark within hours to days. [12] Despite the diversity of these functions, however, the practical potential of azobenzene-functionalized NPs has significantly been limited by the fact that the above self-assembly scheme can only `operate in hydrophobic solvents.[10] So the development of light responsive, dynamic nanoparticle assembly which can function in water medium can lead various important applications like, drug delivery. [15] Light responsive, dynamic assembly has been demonstrated as stimuli responsive drug delivery system in the subsequent section of this chapter.

Since from the earlier experiments in chapter-2 we have seen dynamic nanoparticle system provide stimuli responsive released profile of drug by ADA; we have made this system responsive to light by careful design of ADAPC (1-(2-nitrophenyl)ethyl-adamantane-1-ylcarbamate) molecule. We modified ADA molecule by attaching photocleavable group to the amine group to make ADAPC. We design the guest molecule in such way that it shows two kinds of binding behaviour with CB[7] before and after light irradiation. Initially ADAPC molecule not able to bind to CB[7] molecule, but when irradiated with light due to cleavage

of PC (photo cleavable group) part ADA molecule get generated, and it can form host guest

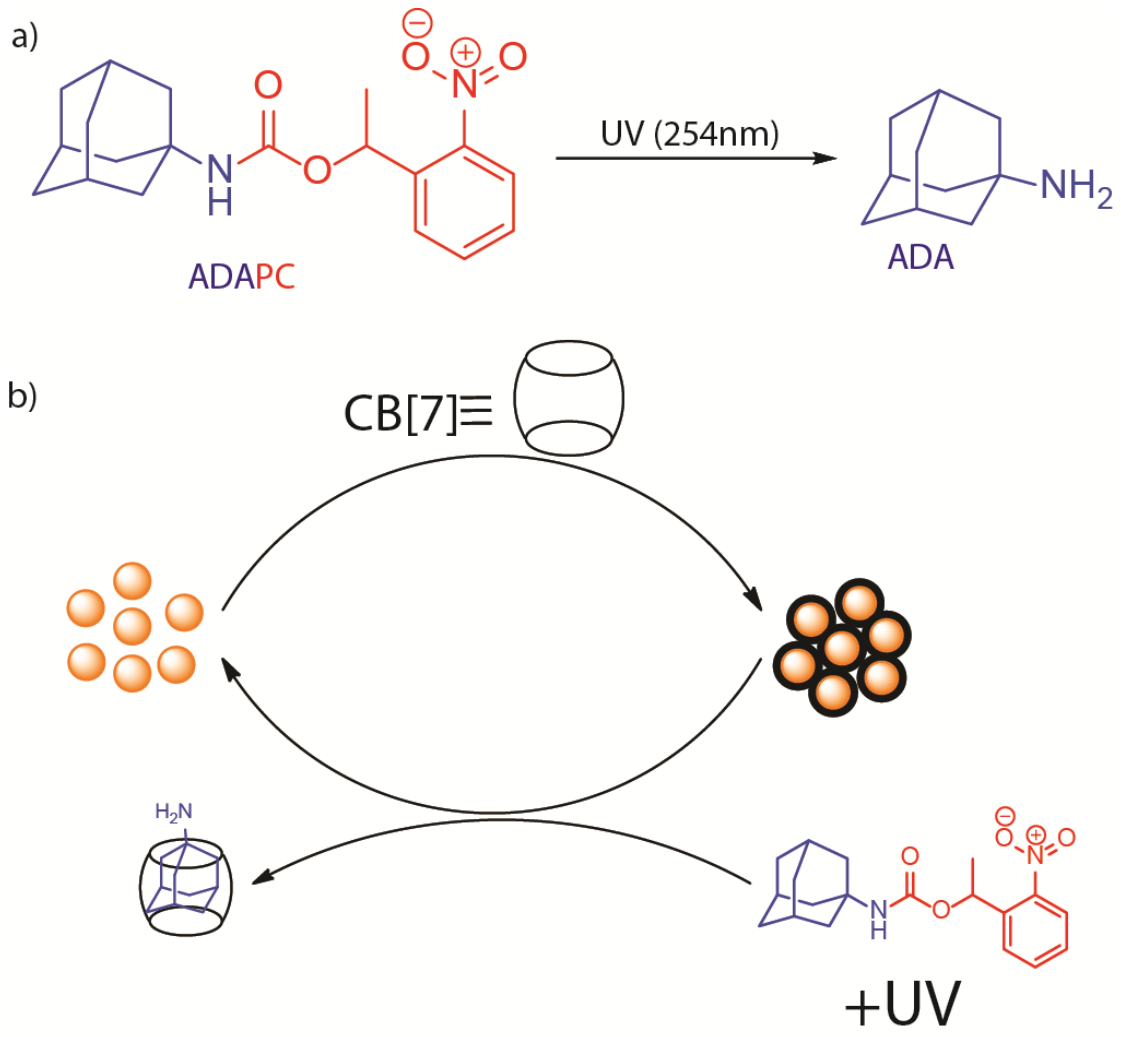

Fig 3.1 | Light triggered disassembly of nanoparticle assembly by ADAPC. a) Light stimulated cleavage of ADAPC molecule to ADA. **b)** CB[7] mediated assembly of nanoparticles and UV-light stimulated disassembly of nanoparticle assembly by ADAPC. In situ generation of ADA molecule leads the disruption of CB[7] molecule by removing CB[7] from nanoparticle surface.

ADA molecule made to ADAPC by reacting NHS-ester of ortho-2-nitrophenyl ethanol(compound2) with ADA. Presence of PC(photocleavable) group in the amine part of the ADAPC restrict the molecule to bind with CB[7] due to steric congestion created by PC group. We use this concept of guest modulation to make the dynamic nanoparticle assembly responsive to light when the light generates ADA molecule from ADAPC and in situ generated ADA molecules leads the assembly to disrupt. Once the assembly gets disrupted drug encapsulated also released in faster rate compared to the control released, so leads the triggered release of the drug. By this concept of guest modulation and alternating interaction with CB[7], we have made light responsive, dynamic nanoparticle assembly. Further drug released study was done using this system, and we tried to establish this concept in cell culture.

3.2 Result and discussion

3.2.1 Photo cleavage study of ADAPC

The study aims to assess the cleavage of ADAPC molecule on irradiation of UV light. UV-Visible spectra were monitored over after a duration of 30 sec exposure of UV light (254 nm, intensity 5 milli watt) for the photo cleavage study of the ADAPC molecule. After UV irradiation absorbance peak around 260 nm started to decrease and a new peak around the 320 nm appears due to the generation of

ketone compound by cleavage of ADAPC molecule. AS the irradiation time increases intensity corresponding to ADAPC (260 nm) decreases and intensity corresponding to ketone compound (320 nm) increases, correlates the fact that ADAPC is continuously cleaving to produce ADA and ketone compound.

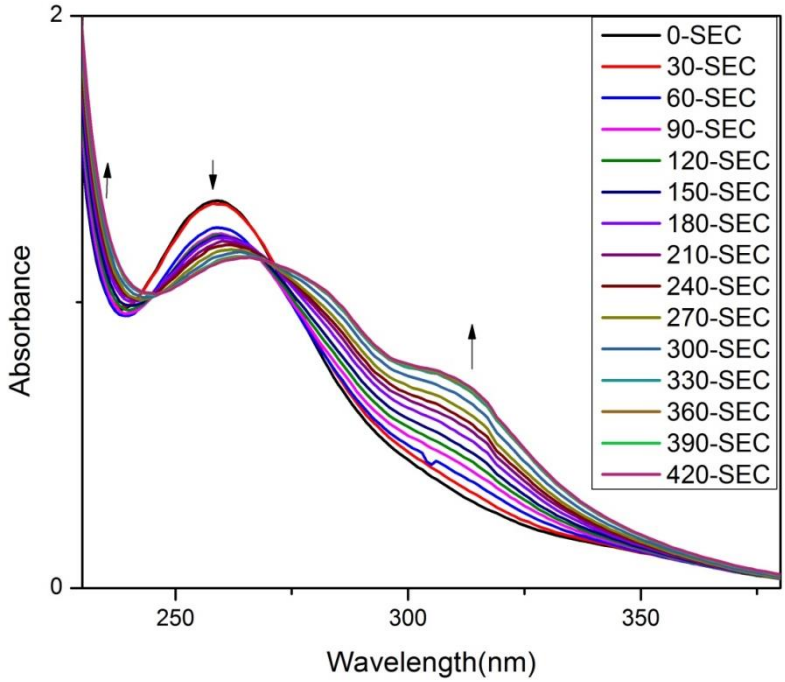

Fig 3.2 | UV-Vis spectral changes upon irradiation with UV light (λ= 254 nm) of ADAPC.

3.2.2 Light-stimulated disassembly of nanoparticle assembly by ADAPC

After a photocleavage study of the ADAPC molecule, we were interested in studying the effect of this photocleavage generation of ADA on CB[7] mediated assembly of gold nanoparticles. To study whether the light can be able to disassembly NP-CB[7] complex first, we make the assembly in a glass vial and then put the ADAPC molecule into the vial an irradiated with UV light. Two set of assembly was made containing ADAPC, set which was irradiated with UV light nanoparticles get dispersed but set which was not irradiated with UV light does not changes (Fig 3.3). In control, nanoparticle was irradiated with UV light but does not show any changes as it is non-photo-responsive (Fig 3.3). This experiment successfully demonstrates the light-stimulated disassembly of nanoparticle assembly.

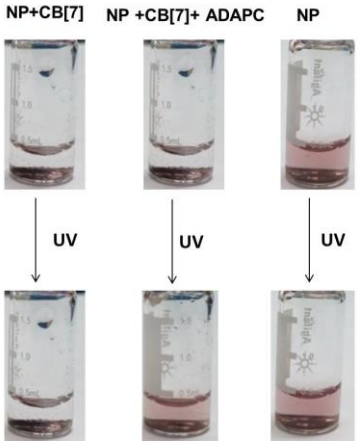

Fig 3.3 | Images of light triggered disassembly of NP-CB[7] complex. Assembly treated with UV irradiation does not change but in the presence of ADAPC assembly disassembled to dispersed state of nanoparticles. The only nanoparticle does not show any changes in UV irradiation.

3.2.3 Light triggered DOX release

Next, we studied the light triggered drug release from the nanoparticle assembly. AS from the fig 3.3, we can say that nanoparticle are getting disassemble by light irradiation so drug molecules inside this assembly can be released on triggered fashion by on-demand applying of light as stimuli. For the drug release study, DOX and ADAPC were encapsulated inside the assembly in the ratio of C_{NP}:C_{DOX}=1:300, C_{NP}:C_{ADAPC}=1:6000. The assembly containing this molecule was transferred inside the implant and dipped into the 1ml PBS in a 24 well plate.Then for the triggered release, UV light of 50 milli watt intensity was irradiated for 60 sec. The fluorescence intensity of DOX was monitored to measure the released of DOX form the implant, increase in fluorescence intensity was observed at 90-minute time point for light triggered set, proof the fact of triggered release DOX. As the nanoparticle assembly containing ADAPC, UV light irradiation cleaves the molecule to ADA, and this in-situ generated ADA molecules form the supramolecular host-guest complex with CB[7]. Nanoparticle assembly get disrupted as CB[7] is captured by high-affinity guest ADA, so encapsulated DOX molecules get diffuse in faster rate into the diffusing media. On the other hand, implant not irradiated with UV light shows normal diffusion of DOX molecule from the nanoparticle assembly.

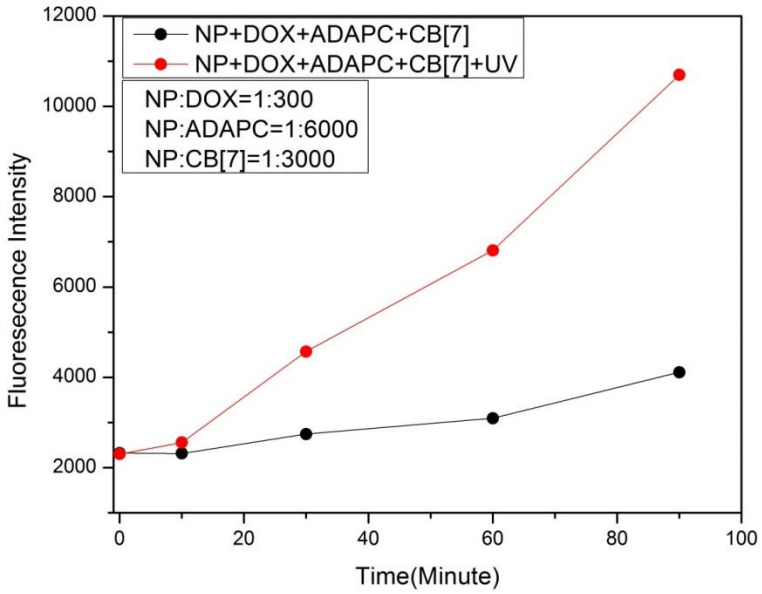

Fig 3.4 | Light stimulated triggered the release of DOX from SDR. The triggered set was irradiated with 254 nm UV of intensity 50 milli watt for 60 sec.

3.2.4 Cell culture study

We next evaluated the DOX and ADAPC encapsulated nanoparticle assembly as a light stimulated drug delivery system through cell culture studies. Assembly contains DOX as drug and ADAPC as stimulant put into the implant and which was then placed on the cell culture plate. Triggered set of the implant was irradiated with a UV light of 254 nm of intensity 50 milli watt for 60 sec; implant was removed after 90 minutes after irradiation. Then cells were kept for 24 hours incubation after 24 hours of incubation cell viability was quantified by Alamar blue assay. Enhanced cytotoxicity was observed for the light triggered set. In

contrast, when the assembly does not irradiate with light show less cytotoxicity.A small percentage of the cell was found dead in case of cells only irradiated with UV light and the implant containing AuBz NP-CB[7] complex irradiated with UV light. These observations demonstrate that dynamic nanoparticle assembly serves as a light stimulated drug delivery system.

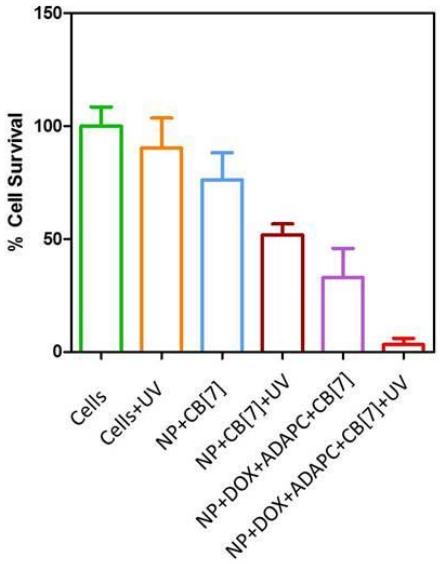

Fig 3.5 | Light stimulated DOX release in cell culture. Hela cell was treated with different conditions like the only UV, NP+CB[7], NP+CB[7]+UV, NP+DOX+ADAPC+CB[7], NP+DOX+ADAPC+CB[7]+UV. Enhanced cytotoxic-city was observed for NP+DOX+ADAPC+CB[7]+UV set compare to the other conditions as NP+DOX+ADAPC+CB[7] and NP+CB[7]+UV**.**

3.3 Conclusion

In summary, we have demonstrated a novel, light controlled drug delivery system, based on dynamic nanoparticle assembly. The release mechanism appears to involve disruption of the nanoparticle assembly by photoinduced photodegradation and instantaneous generation of ADA from ADAPC molecule. Experimental results have shown that upon exposure to UV light, the ADAPC molecule inside the assembly undergo degradation and generates ADA molecule breaks the assembly and leads the faster release of DOX. Proposed strategy can be considered as a new platform for the photostimulated drug delivery systems that offer the possibilities of the controlled delivery of wide variety of drugs. However, cell culture result is not very well and not showing same trends in reproducibility and a very wide separation in cytotoxicity for the triggered set and controlled set. We will try this system to make better by further studies in future. So we can say we work to demonstrate a multi stimuli (small molecule and light) based drug delivery system based single component dynamic nanoparticle assembly where bio orthogonal supramolecular interaction of CB[7]-ADA pair play key role in making the process dynamic.

3.4 Experimental section

3.4.1 Materials and methods

All the chemicals were purchased from Sigma Aldrich, Alfa Aesar or TCI India. Dichloromethane was dried according to the standard procedure. ^{1}HNMR spectra were recorded in Bruker AVANCE 400 FT-NMR spectrometer with chemical shifts reported in parts per million (ppm) with respect to Tetramethylsilane (TMS).

3.4.2 Synthesis and characterization

Synthesis of PC, PC-NHS and ADAPC

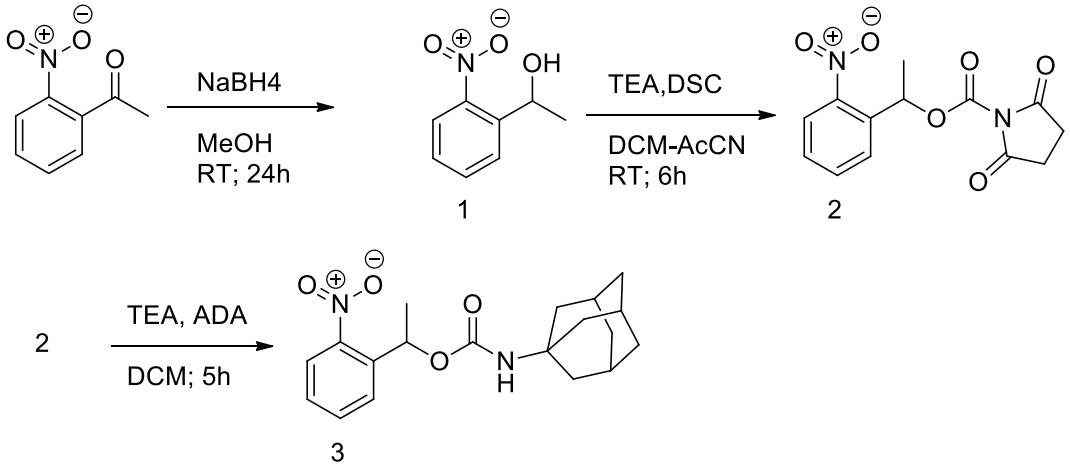

Synthesis of Compound 1 (PC): 1-(2-nitrophenyl) ethanone (400 mg; 2.42 mmol) was dissolved in 10 ml HPLC grade methanol. $NaBH_4$ (366 mg; 9.68 mmol) was slowly added to the soln by keeping the R. B. flask in the ice-cold condition; ice was removed after and then stirring for 16 h at room temperature.

After completion of the reaction, the solvent was evaporated by using rotary evaporator. Then water was added to the reaction mixture and extracted three times using ethyl acetate. The organic layer was combined, dried over Na_2SO_4 and solvent was removed by rota evaporator and dried in vacuum to get the product.Yield 90%. ^{1}H NMR ($CDCl_3$, 400 MHz): δ 7.93-7.80 (m, 2H), 7.68-7.62(t, 1H), 7.45-7.39(t, 1H), 5.46-5.38(q, 1H), 2.28(br, 1H), 1.58-1.55(d, 3H).

Synthesis of Compound 2 (PC-NHS): Compound 1 (1.3 g; 7.7 mmol) was dissolved in 10 ml AcCN-DCM (1:1) dry solvent under a nitrogen atmosphere. Then TEA(3.24 ml; 23.31 mmol) was added to the reaction mixture. Then DSC (5.97 gm; 23.31 mmol) was added to the reaction mixture and kept for stirring for 6 hours. After 6 hours of reaction, volume was made 30 ml by adding DCM to the reaction mixture. Then 20 ml 1(N) HCl was added and extracted by using separating funnel. The aqueous layer was removed and again extracted with 20 ml saturated NaCl soln. Again the aqueous layer was removed, and DCM layer passed over anhydrous Na_2SO_4. The solvent was removed by rota evaporator, and the crude reaction mixture was obtained. Then the mixture was purified by flash chromatography using hexane-ethyl acetate as the solvent system. Yield 70%. ^{1}H NMR ($CDCl_3$, 400 MHz): δ 8.04-7.99(d, 1H), 7.76-7.71(m, 2H), 7.52-7.47(m, 1H), 6.42-6.36(q, 1H), 2.79(s, 4H), 1.80-1.77(d, 3H).

Synthesis of Compound 3 (ADAPC): ADA (50 mg, 0.33 mmol) was dissolved in 2 ml of dry DCM in 25 ml round bottom flask. Then TEA (0.134 ml, 0.99 mmol) was added to the round bottom flask. Finally, compound 2 (101 mg, 0.33 mmol) was added and kept for stirring for 5 hours. After the 5 hours, DCM was removed by rota evaporator, and the crude mixture was obtained. The crude mixture was again dissolved in 5 ml DCM and extracted with water in the separating funnel. DCM layer was collected and dried and then purified by flash chromatography. Yield 50%. ^{1}H NMR ($CDCl_3$, 400 MHz): δ 7.98-7.88(m, 1H), 7.67-7.56(m, 2H), 7.45-7.35(m, 1H), 6.26-6.15(q, 1H), 4.66-4.53(br, 1H), 2.05(m, 3H), 1.93-1.90(d, 3H), 1.69-1.52(m, 12H).

3.4.3 Photocleavage study of ADAPC molecule

0.22 mM 400 µl soln of ADAPC was made in a mixture solvent of H_2O:AcCN (50:50). For the photocleavage study soln was taken in a two-sided black cuvette and irradiated with a UV source of 5 milli watt from through the transparent side of cuvette wall. The measurement was done after every 30 sec of UV irradiation.

3.4.4 Assembly preparation for light triggered DOX released

For the light triggered DOX released study assembly was made in the ratio of C_{NP}:C_{DOX}=1:300, C_{NP}:C_{ADAPC}=1:6000,C_{NP}:$C_{CB[7]=}$1:3000. At first 37.1 µl of 4.04 µM soln of 4 nM 4 nm benzyl nanoparticle soln was taken in 500 µl Eppendorf tube, and then 18 µl of 2.5 mM DOX and 4.96 µl of 181 mM ADAPC soln was

added to the Eppendorf tube and mixed properly. To make the assembly of this mixture 22.5 µl of 20 mM CB[7] was added to the mixture. After instantaneous assembly formation Eppendorf tube was centrifuged for 1 min 50 rpm and the supernatant was removed, further washed with 50 µl PBS soln. Then assembly was transferred inside the implant (dipped into 1 ml PBS soln in 24 well plate) by 100 µl PBS. For trigger action trigger set was irradiated with UV light for 60 sec of intensity 50 milli watt from the top of the implant. The fluorescence measurement was started to monitor the DOX release by taking 70 µl PBS from the well plate, and measurement was done in plate reader in the corning black well plate. Excitation for the DOX was 480 nm, and emission was collected at 570 nm.

3.4.5 Cell culture study

Cells were plated as earlier mentioned in chapter2. Then further treatment of cell was done as mentioned in 3.2.4 section.

References

1. Yun, Y. H., et al. Controlled Drug Delivery: Historical perspective for the next generation. *J Control Release*. **2015**, *219*: 2-7.

2. Park, K. Controlled drug delivery systems: past forward and future back. *J Control Release.* **2014**, 190: 3-8.

3. Agasti, S. S., et al. Photoregulated Release of Caged Anticancer Drugs from Gold Nanoparticles. *Journal of the American Chemical Society.* **2009**, *131*(16): 5728-5729.

4. Brudno, Y. and D. J. Mooney. On-demand drug delivery from local depots." *Journal of Controlled Release.* **2015**, *219*: 8-17.

5. Bansal, A. and Y. Zhang. Photocontrolled Nanoparticle Delivery Systems for Biomedical Applications. *Accounts of Chemical Research.* **2014**, *47*(10): 3052-3060.

6. Blum, A. P., et al. (2015). Stimuli-Responsive Nanomaterials for Biomedical Applications. *Journal of the American Chemical Society.* **2015**, *137*(6): 2140-2154.

7. Mura, S., et al. Stimuli-responsive nanocarriers for drug delivery. *Nature Materials.* **2013**, *12*: 991.

8. Karimi, M., et al. Smart Nanostructures for Cargo Delivery: Uncaging and Activating by Light. *Journal of the American Chemical Society.* **2017**, *139*(13): 4584-4610.

9. Rotello,V. M., Gold nanoparticles in chemical and biological sensing. Chemical reviews, **2012**, *112* (5), 2739-2779.

10. Samanta, D. and R. Klajn. Aqueous Light-Controlled Self-Assembly of Nanoparticles. *Advanced Optical Materials*. **2016**, *4*(9): 1373-1377.

11. Manna, D., et al. Orthogonal Light-Induced Self-Assembly of Nanoparticles using Differently Substituted Azobenzenes. *Angewandte Chemie International Edition.* **2015**, *54*(42): 12394-12397.

12. Kundu, P. K., et al. Light-controlled self-assembly of non-photoresponsive nanoparticles. *Nature Chemistry*. **2015**, *7*: 646.

13. Das, S., Dual-Responsive Nanoparticles and their Self-Assembly. *Adv. Mater.* **2013**, *25*, 422–426.

14. Kundu, P. K., et al. Controlling the lifetimes of dynamic nanoparticle aggregates by spiropyran functionalization. *Nanoscale.* **2016**, *8*(46): 19280-19286.

15. Li, F., et al. Dynamic Nanoparticle Assemblies for Biomedical Applications. *Advanced Materials.* **2017**, *29*(14): 1605897.